Applications of *p*-hydroxyphenacyl (*p*HP) and coumarin-4-ylmethyl photoremovable protecting groups[†]

Richard S. Givens[a], **Marina Rubina**[b], and **Jakob Wirz**[c]

Richard S. Givens: givensr@ku.edu; Marina Rubina: mrubin3@ku.edu; Jakob Wirz: J.Wirz@unibas.ch

[a]Department of Chemistry, University of Kansas, Kansas, USA; Tel: +1 785 864 3846

[b]Department of Chemistry, University of Kansas, Kansas, USA; Tel: +1 785 864 1574

[c]Department of Chemistry, Klingelbergstrasse 80, CH-4056 Basel, Switzerland; Tel: +41 76 413 47 48

Abstract

Most applications of photoremovable protecting groups have used *o*-nitrobenzyl compounds and their (often commercially available) derivatives that, however, have several disadvantages. The focus of this review is on applications of the more recently developed title compounds, which are especially well suited for time-resolved biochemical and physiological investigations, because they release the caged substrates in high yield within a few nanoseconds or less. Together, these two chromophores cover the action spectrum for photorelease from >700 nm to 250 nm.

Introduction

o-Nitrobenzyl derivatives are by far the most commonly used photoremovable protecting groups (PPGs),[1] despite their known disadvantages: following electronic excitation, the caged compounds are released on a time scale of microseconds at best,[2] and *o*-nitroso aromatic ketones are produced as side products, which usually absorb more strongly than the parent PPG at the irradiation wavelengths and which may interfere with the effect of the released bioactive material under study, because of their toxic effect on biological tissues.[3] With the need for higher time resolution in studies of the leading events in biological processes, there is a demand for clean, rapidly released triggers or initiators of these processes.

The technology to monitor events on the nanosecond to femtosecond time scales has become available and to exploit these methods the initiating processes must match or exceed the rates of detection. Recent advances in time-resolved Fourier transform infrared (TR FTIR) and attenuated total reflectance (TR ATF), for example, permit investigations of protein binding and enzyme catalysis at the nanosecond level.[4] This review focuses on relatively recent additions to the PPG variety, *p*-hydroxyphenacyl (*p*HP)[5] and coumarylmethyl derivatives,[6] which offer an alternative to *o*-nitrobenzyl.

p-Hydroxyphenacyl photoremovables (*p*HP)

Anderson and Reese discovered the molecular reorganization that occurs upon irradiation of *p*HP chloride.[7] The mechanism of the photochemical release of the leaving group (LG) from *p*HP diethyl phosphate (**1**) in aqueous solution is summarized in Scheme 1.[8] Release of a

---

[†]This paper is part of a themed issue on photoremovable protecting groups: development and applications.

Correspondence to: Richard S. Givens, givensr@ku.edu.

typical caged substrate upon irradiation in neutral aqueous solution at λ = 250–350 nm cleanly and efficiently proceeds through its triplet excited state forming a putative spirodiketone **2**, termed the Favorskii intermediate. The spirodiketone is subject to hydrolytic ring opening yielding *p*-hydroxyphenylacetic acid (**3**). The structural rearrangement closely follows the classical ground state Favorskii rearrangement of α-haloketones, hence the origin of its moniker as the "photo Favorskii rearrangement". In contrast to the starting material, the photoproducts **3** (and traces of **4**) are essentially transparent at wavelengths above 290 nm.

Leaving group effects

As a general rule, the most efficacious leaving groups are those with a pK_a < 11. Alcohols and primary, secondary, and tertiary amines with pK_a's above the threshold of 11, with a few exceptions,[9] have not been successfully released from *p*HP cages although little has been reported on these functional groups (*vide infra*).

Several studies have shown that the *p*HP triplet lifetimes, $^3\tau$, and the rate constants for release, $k_{rel} = \Phi_{dis}/^3\tau$, depend on the leaving group pK_a.[10–13] As shown in Table 1, for pK_a's that range from the reactive mesylate (−1.54) and tosylate (−0.43) to the less efficient phenols (8–11) and thiols (~8) give a range of rate constants k_{rel} that spans three orders of magnitude and quantum yields that vary by a factor of 20.

The dependence of the rate constants k_{rel} on the pK_a's of the LGs is demonstrated by a Brønsted linear free energy relationship, $\log(k_{rel}/s^{-1}) = (9.57 \pm 0.14) - (0.24 \pm 0.03)pK_a$, *i.e.*, $\beta_{LG} = -0.24$ (Fig. 1). This correlation implies significant heterolytic bond breaking at the transition state for release.

Laser flash transient absorption studies have detected the allyloxy–phenoxy biradical intermediate shown in Scheme 1, which intervenes between the excited triplet and the "Favorskii" intermediate.[8] The biradical triplet results from the extrusion of both a proton and the leaving group anion from the triplet ketone ^{3}**1**. This indicates that the leaving group departs in its ground state since spin conservation requires only one triplet species be formed if the reaction is concerted. The simultaneous departure of both the proton and the leaving group is further supported by the observation of a solvent kinetic isotope effect (SKIE k_{H_2O}/k_{D_2O} = 2.17).[8] The Brønsted $\beta_{LG} = -0.24$ for the photochemical reaction finds precedence in gas-phase collision-induced dissociation (CID) fragmentation measurements of the conjugate base of the *p*HP derivatives in Table 1.[12] A correlation coefficient of $\beta_{LG} = -0.19 \pm 0.02$ for the appearance energies (AEs) *vs.* gas-phase acidities of the leaving groups ($-\Delta H_{acid}$) reveals a similar extent (19% *vs.* 24%) of bond breaking at the transition state for the fragmentation process.

Chemical yield

An ideal PPG should give a quantitative yield of the unprotected functional group. Moreover, the irradiation dose required should be minimal to avoid unwanted photochemistry such as photoreactions of the products. Meeting these objectives avoids deleterious processes that compromise the efficacy of PPG-based methods. Poor chemical yields of released material, secondary photochemical reactions and over-irradiation leading to degradation of products and spectator components of the reaction mixture often result in complex mixtures of unwanted materials. For the *p*-hydroxyphenacyl derivatives, both criteria are met since the conversions are spectacularly clean and the quantum efficiencies approach unity.

Stability to thermal degradation

Esters, phenyl ethers and thio ethers of *p*HP are very stable in organic solvents. Most esters and all ethers are also stable in aqueous-based solvents at neutral pH and do not undergo hydrolysis at ambient temperatures. However, as the leaving group reactivity increases, *e.g.*, sulfonate leaving groups, the caged compound's stability decreases. Aqueous solutions of carboxylate esters may undergo slow hydrolysis at room temperature over a 24 h period forming the α-hydroxyketone. The rate of hydrolysis increases at higher pH (>9). No rearrangement products are detected, and thus no ground-state Favorskii rearrangement takes place under these basic conditions.[14]

Selected applications of *p*HP derivatives

The *p*HP PPG has been successfully deployed for time-resolved biochemical and physiological studies to delineate response kinetics,[15] or to define spatial resolution in tracking signal transduction in neural networks.[16] Several of these applications have been reviewed earlier.[15] More recently, time-resolved absorption spectroscopy,[8,14,17–20] Fourier transform IR (TR-FTIR)[3,4,21] and resonance Raman (TR[3]),[10,22,23] techniques have become available for better time-resolved applications in biological chemistry, such as examining substrate binding, enzyme conformational changes, dynamic inhibition and signal transduction kinetics. Several applications have incorporated an initiating *p*HP photo-activation step, again taking advantage of *p*HP's rapid release rate.

The *p*HP phosphate derivatives are most frequently deployed for studies on enzyme catalysis, such as the photo-initiation step for kinetic studies,[3,24] taking advantage of their very rapid and clean phosphate group release.[3–5,10,18–24] For carboxylate release, such as the C-terminus of amino acids, peptides, and oligopeptides, the value has been in their ease of synthesis, clean, high yielding release, and biological compatibility. Bradykinin, L-glutamate, and GABA have been employed for several *in vitro* and *in vivo* studies, *e.g.*, to activate the BK_2 receptor, and as agonists or antagonists in mouse neuroreceptor stimulation studies of the auditory system.[15,16] Assorted applications of *p*HP thio derivatives that take advantage of the high nucleophilicity of thiol for direct incorporation of the protecting group using *p*HP Br have been reported.[25,26]

The first examples of *p*HP phosphate release came from the investigations by Fendler *et al.*[24] on ATPase hydrolysis of Na^+, K^+-ATP and at about the same time by Du *et al.*[3,27] on *p*HP GTP as an initiator of the catalytic hydrolysis of GTP by Ras protein–GTPase. These two hallmark applications demonstrated the power of *p*HP as a phototrigger for the rapid release of the nucleotides ATP and GTP, in contrast to more commonly employed *o*-nitrobenzyl (*o*NB) and *o*-nitrophenylethyl (*o*NPE) PPGs. Fast cage release of the nucleotides was crucial for determining rate constants of the earliest events in a catalytic hydrolysis. In Du *et al.*'s work,[27] kinetic isotope effects obtained from the rates of hydrolysis of ^{18}O-labeled α-, β-, and γ-phosphates of GTP were determined from time-resolved FTIR analyses of the rates of bound and free phosphate. The changes in binding of GTP in the catalytic pocket during its hydrolysis of GDP were determined using ^{18}O-induced spectral shifts from photolysis of the three *p*HP ^{18}O-labelled GTP isomers. An increase in β-phosphate binding coupled with prior evidence of deprotonation of the γ-phosphate led the authors to conclude that hydrolysis occurs through a dissociative mechanism forming *meta*-phosphate intermediate and GDP. Rapid H_2O addition to the *meta*-phosphate yields inorganic phosphate ($H_2PO_4{}^{2-}$, P_i), which is then released from the catalytic site in the rate-determining step. These studies relied heavily on the rapid release rate of *p*HP GTP to monitor the initial rates for binding at the catalytic site and to confirm its location (*vide infra*). Attempts to perform the same experiments using *o*NPE GTP were unsatisfactory and

resulted in the early onset of extraneous IR signals masking the slower evolution of signals associated with the changes in binding from GTP to GDP.

In a follow-up communication,[3] Du *et al.* documented the source of the difficulties encountered with the *o*NPE GTP study. The *o*NPE photolysis byproduct results from a photoredox reaction of the chromophore forming an α-nitrosoacetophenone. Nitroso ketones and aldehydes are the common byproducts for all *o*-NB-based caged compounds and are very susceptible to nucleophilic attack by amines and thiols. To counteract this effect, a common practice has been to add dithiothreitol (DTT) to the photolysis mixture in order to trap or disable any aryl-nitroso by products. Spurious signals that appeared early in the *o*NPE GTP photolysis were shown to arise from reactions of nitrosoacetophenone with the protein. In the absence of protein, the nitrosoacetophenone is readily detected.

The rate of *o*NPE cage release is also many orders of magnitude slower than that of the *p*HP analogs: k_{rel} = 1.0–10 s^{-1} (*o*NPE)[2] *vs.* 10^8–10^9 s^{-1} (*p*HP).[8,17,22] The vital time frame required for RasGTP catalysis by TR-FTIR was too fast for *o*NPE GTP initiation.[3,4] The initial TR-FTIR fingerprints of the binding changes of the α- and β-phosphate groups on GTP were only observed with labelled *p*HP GTP as phototriggers.[3,21,28,29]

A similar comparison of TR-FTIR analyses of *p*HP ATP and *o*NB ATP-catalyzed hydrolysis was reported by Fendler *et al.*[24] Here, the authors reached the same conclusions regarding the quality of data using the two methods for triggering the hydrolysis. Benzoin-protected ATP was also examined but did not provide useful results, primarily due to fluorescence and competition for incident radiation by the phenylbenzofuran photoproduct.

Gerwert *et al.*[21] extended the TR-FTIR technique by developing it into a rapid high-throughput screening method as a competitive drug–protein binding assay. Using TR-FTIR difference spectra to tease out the changes in GTP–GDP binding in the presence and absence of small molecular weight pharmaceutical candidates, the degree of inhibition at key functional groups on the protein and/or induced changes in the protein's conformation are measurable. The "on" and "off" signalling can be automated for high-throughput screening, a novel application of caged compounds with even broader applications for pharmaceutical drug development.[30] This approach may be useful in assaying information about the active binding site of potential GTPase inhibitors.

Kötting *et al.*[4,28] also determined the kinetic parameters and activation energies for GTP hydrolysis by GTPase in water and catalyzed by the Ras protein-GTPase in order to evaluate the extent of entropic *vs.* enthalpic influence of the protein on the catalytic cycle. Ras increased the rate of hydrolysis by 10^5 relative to H_2O and 10^7 when Mg^{2+} was present in the aqueous solution. Temperature dependent rates showed that the $\Delta\Delta H_0^*$ of 5.2 kcal mol^{-1} for water *vs.* RasGTP was essentially the total source of the diminished activation barrier to the hydrolysis. The $T\Delta\Delta S_0^*$ value was less than 0.5 kcal mol^{-1}, essentially demonstrating that the protein was not providing enhanced ordering at the transition state in the hydrolysis process.

These values were determined using ^{18}O frequency shifts at 1143 cm^{-1} for RasGTP and 1114 cm^{-1} for RasGDP to register the rate of formation of the RasGTP complex and its hydrolysis upon photolysis of *p*HP GTP. The frequency shifts for the α and γ labelled phosphates showed an upshift in comparing the GTPase activity in H_2O *vs.* with protein-bound RasGTPase. The β-phosphate caused a downshift indicating a build-up of negative charge density at that position in accord with the earlier findings of Du *et al.*[3] This was accounted for by the proximity of the Mg^{2+} ion and Lys16 near the β phosphate to encourage negative charge migration to the phosphate oxygen through electrostatic attraction (Fig. 2).

It should be pointed out that the synthesis of ^{18}O-labeled phosphates of nucleotides like ATP and GTP is readily accomplished since the synthetic strategy for pHP caged phosphates simply involves the condensation of labelled pHP OPO(OH)$_2$ with the mono- or diphosphorylated nucleoside bases (Scheme 2).[3–5,15]

Wittinghofer, Gerwert, Kötting, and coworkers have made important contributions to unveiling the specificity of Ras and Rap, two GTPase activating proteins (GAPs) that assist in catalytic hydrolysis of GTP.[4,29,31,32] Subtle changes in the amino acid sequence and mutations can greatly affect the GTP and GDP binding and hydrolysis of GTP by RasGTPase altering the "on"–"off" signalling by the enzyme, which is considered one of the major determinants in uncontrolled cell growth.[4]

Regulation of phosphotyrosines, important in transmembrane signalling, is governed by the competitive rates of formation and hydrolysis of tyrosine phosphates. The analysis of the rates of phosphotyrosine formation by phosphotyrosine phosphatase (PTP) has been the target of several mechanistic investigations including small molecule inhibition. The hydrolysis of tyrosine phosphate involves the intervention of a neighbouring cysteine at the active site which attacks the phosphate forming a cysteine thiophosphate intermediate that is hydrolyzed to P$_i$. α-Haloketone derivatives including phenacyl halides act as small molecule inhibitors that block this pathway by reacting covalently with the cysteine thiol as "suicide inhibitors".

Pei and coworkers[33] showed that pHP Br inhibited PTP hydrolysis by reaction with the key cysteine (Cys 453) located at the enzyme active site. For PTP SHP1(ΔSHP2) the "suicide inhibition" was complete in a few minutes ($k_{inact} = 0.40$ min^{-1}) which could be replicated in human B cells. In this case, inhibition was shown to cause protein hyperphosphorylation. Unlike traditional "suicide inhibitors," Pei's work demonstrated that the pHP thio ether linkage could be severed from the enzyme photo-chemically at 350 nm. Up to 80% of the PTP SHP1(ΔSHP2) activity was restored with a 15 min exposure, providing a model for mechanistic investigations of "on"–"off" inhibition of enzyme catalysis and other fast kinetic studies at cysteine active sites.

Goeldner[25] has further demonstrated that pHP thioethers undergo the same rearrangement as the ester counterparts to give 90% of the rearranged p-hydroxyphenylacetate products along with ~10% of p-hydroxyacetophenone, suggesting a small radical component for this reaction. In fact, the release of the thiol leads to disulfide dimers in ~70% yields with a quantum yield of 0.085 for 3′-thio-dTMP in Tris–HCl buffer (pH 7.2). No attempts were made in this study to suppress radical coupling reactions with citrate or other moderators. An interesting variant in the product mixture was 30% formation of p-hydroxyphenylacetate thioester **6**. Its formation may be the result of nucleophilic addition by the released thiol (pK_a = 8.4) to the spirodiketone **5**, which then opens to **6** (Scheme 3).

Three thiol derivatives (*N*-benzylcysteine, 3′-thio-deoxythymidine phosphate (3′-thio-dTMP, a substrate analog for thymidilate monophosphate kinase), and glutathione) were pHP "protected" by direct displacement on pHP Br with the thiols in 80–90% yields. The ease of thiol protection–deprotection by addition of pHP Br followed by photochemical deprotection has served as a basis for several studies on cysteine and thiophosphate substrates.

Bayley *et al.*[26] compared the protection–deprotection effectiveness of *o*NB and pHP for thiophosphorylated tyrosine. Both protection sequences were accomplished in high yield (75% and 90%, respectively) by treatment of the thiophosphorylated tyrosyl peptide

EPOYEEIPILG with oNB Br and pHP Br. Both were equally stable to storage as well as to reaction conditions without light (Scheme 4).

Irradiation at 312 nm released the thiophosphated peptide in 50–70% yields with quantum yields of 0.25–0.37 (oNB) and 0.56–0.65 (pHP). The chemical and quantum yields were pH dependent between pH 5.8 to 7.3, but at pH 8.2 the reactants and/or the products were not stable. Irradiation conditions at 312 nm resulted in deprotection from pHP ten times faster than from oNB due primarily to a combination of higher efficiency and larger absorptivity for pHP at this excitation wavelength. Both deprotection reactions provided the oligopeptide regaining 50–70% of its original binding capacity as determined by radio-labelled binding studies with recombinant SH2 domain.

Bayley et al.[26] extended this approach to the protection–deprotection of thiophosphorylated threonine, Thr-197, in the catalytic site of a cell-signalling protein kinase A found in the catalytic C_α subunit by phosphorylation. The phosphothreonine unit plays a key role in stabilizing the active conformation of the C_α catalytic subunit. The thiophosphorylated threonine was effectively protected by direct reaction with pHP Br to yield pHP-P_ST^{197} C_α. It is noteworthy that the thiophosphorylated threonine ($pK_a = 5.8$) was selectively protected with pHP Br in the presence of potentially competing cysteine residues. Both the binding capability and the specific activity of the caged enzyme were dramatically reduced, to 2.4% (binding assay measured on TNB-thio agarose beads) and by a 17-fold decrease in ^{32}P kinase activity. Photolysis at 312 nm at pH 7.3 restored 85–90% of the binding activity and the specific activity was nearly recovered (15-fold increase) with a quantum yield of 0.21. The role of the pHP group in this instance is to block or diminish H-bonding and electrostatic attractions between the threonine-197 and Arg-165 with Lys-189, the amino acids that stabilize the closed form of the C_α subunit.

Protecting groups have a long history of application, which takes advantage of the ability to control the exposure of reactive functional groups to reactive environments during multistep syntheses of peptides, nucleotides and polymers.[34] While photoremovable caged compounds have long been considered for applications in these areas, related applications on solid surfaces[35] are receiving more attention. Three attractive characteristics for photochemical approaches toward systematic exposure of functional groups are the location and the density of the exposed functionalities. Added to this is the temporal control which can be important for investigations of signal processing. These attributes have encouraged an explosive array of applications[36] and surface-bound caged compounds have been exploited for controlled exposure of groups such as carboxylic acids, amines, thiols, and many other reactive functional groups bound to glass surfaces, beads, polymeric supports, and other solid surfaces.

Photoremovable protecting groups applied to regulation of PCR and gene expression have been explored with mixed results. Many attempts to control polynucleotide selectivity and activity using PPGs have also been attempted.[37] However, a recent study by Pickens and Gee[9] has opened a potentially useful new application using pHP protection of the 3′-hydroxy group on thymidine that, as its corresponding phosphoramidite, could be employed in PCR. In this study, the 3′-hydroxy was protected as its pHP ether. Photolysis of pHP **7** released thymidine quantitatively in 15 s (Scheme 5). The authors suggested that the protected phosphoramidite might serve as a photoreversible blocker for selective PCR modification of the nucleotide array (Fig. 3).

(Coumarin-4-yl)methyl [coumarylmethyl] photoremovable protecting groups

The development of coumarylmethyl cages as a new class of photoremovable groups commenced with the discovery by Givens and Matuszewski of the photoreactivity of a coumarinylmethyl group in releasing phosphate ester **8** (Scheme 6).[6]

Schmidt and coworkers[38] have probed the mechanism of release from several coumarylmethyl cages CM–LG using quantitative quantum yield and time-resolved measurements of the photochemistry and fluorescence of coumarylmethyl esters and the corresponding alcohols (*vide infra*, Scheme 14 and Table 3). Heterolytic bond cleavage, k_{cl}, proceeds from the relaxed excited singlet state ^{1}CM–LG* in competition with fluorescence and nonradiative decay processes, k_f and k_{nr}, forming a singlet ion pair ^{1}[CM$^+$…LG$^-$] in the initial reaction step (Fig. 4). Escape from the solvent cage first affords the solvent-separated ions CM$^+$ and LG$^-$. The coumarylmethyl cation CM$^+$ reacts with water to yield the product alcohol CM–OH and H$^+$ in addition to the leaving group anion LG$^-$.

The cleavage rate constants, k_{cl}, were estimated from measurements of the fluorescence quantum yield, Φ_{fl}, and the fluorescence lifetime, τ_{fl}, of the alcohols CM–OH and the fluorescence and photochemical quantum yields, Φ_{fl} and Φ_r, of the coumarylmethyl esters CM–LG. The resulting rate constants k_{cl} range from 0.1 to 50×10^9 s^{-1} and obey a linear free energy relationship with the acidity constants pK_a of the LG acids, *i.e.*, those releasing the strongest acid are fastest. A similar relationship was found for the heterolytic cleavage from the triplet state of *p*HP esters (Fig. 1). The ratio of escape to recombination from the ion pair could not be determined directly, but the measurements indicated that the factors that accelerate the heterolytic bond cleavage retard the ion recombination reaction.

Coumarin-based PPGs have gained considerable attention, especially for applications in biological chemistry,[39] primarily due to its longer-wavelength absorption, extending farther into the visible region (400–500 nm) and the fast release rate from its excited singlet. These advantages have been offset by coumarin's marginal quantum yields, low aqueous solubility and the occasional inconvenience of a strong fluorescence and competitive absorptivity from the coumarin photolysis byproducts. However, many successful efforts have been reported where clever modifications to the coumarin group have resulted in somewhat higher quantum yields and better aqueous solubility. These, together with adaptations that expand the leaving group range (including alcohols and amines), have raised researchers' awareness to this relatively new class of PPGs.

The first generation of coumarylmethyl cages possessing an –OH or –OMe substituent at C7 were characterized by very fast release rates and great hydrolytic stability. However, they had a drawback of poor solubility and relatively low quantum yields for all leaving groups except phosphates. 6-Bromo-derivatives where designed to lower the pK_a of the 7-hydroxy group by two units to effect a complete deprotonation at physiological pH, thereby enhancing water solubility and causing a bathochromic shift of 60 nm (Table 2). The downside of this modification was the increased susceptibility of some of the bromo-substituted caged compounds to hydrolyze in the dark. Further development in this area resulted in emergence of a second-generation of coumarylmethyl PPGs bearing an amino group at C7, which significantly improved the spectroscopic and photochemical properties of the cage, moving the absorption maxima to 350–400 nm and recording the highest quantum yields among the analogues. Solubility of the aminocoumarylmethyl cages could be improved by appending polar groups such as carboxylates to the aniline moiety. Strong fluorophoric properties, which are even more enhanced in the polyaromatic analogs, lend a convenient tool for monitoring of the reaction course.

Applications of coumarin caged compounds

Phosphates—Photolysis of 4-methoxycoumarylmethyl phosphate was the first example that employed a coumarylmethyl PPG[6] and current literature reveals that coumarinylmethyl phosphates continue to be the most frequently encountered application of the coumarin cage. Most caged phosphates have good stability to hydrolysis (although some analogues may have limited water solubility), adequate quantum efficiencies ($\Phi = 0.03$–0.2), and are easily synthesized, which, taken together with very fast release kinetics, make coumarin-caged phosphates very attractive candidates for biological applications. Depending on specific needs, properties of caged phosphate can be tuned by modifying substituents on the coumarin core. Studies by Lima *et al.* also emphasize the importance of pH control in photolysis of ionizable 4-methylcoumarin-caged phosphates, which show significant dependence of quantum yields on pH variations.[64] A review by Furuta provides useful guidelines for choosing a suitable cage.[65] The most recent applications of caged phosphates in biological studies are described below.

Caged peptide **9** was used as a modular domain-binding peptide in the investigation of PI3K kinase-mediated phosphorylation of proteins. Irradiation of **9** in K-MOPS buffer solution quantitatively produced phosphopeptide **10** and hydroxymethylcoumarin **11** with a quantum yield of 0.12 (Scheme 7).[66] Peptide **10** was also successfully released in living cells upon exposure at 365 nm without causing any toxicity.

Schultz and coworkers demonstrated that 7-diethylaminocoumarin-4-ylmethyl-caged bioactive phosphatidylinositol 3,4,5-triphosphate (PI(3,4,5)P$_3$) can be effectively transported through the plasma membrane and then uncaged to release PI(3,4,5)P$_3$, inducing membrane ruffling and pH-domain translocation in the presence of the PI3-kinase inhibitor wortmannin (Fig. 5).[67] The cell entry by PI(3,4,5)P$_3$ was conveniently monitored by fluorescence microscopy. Biological response was observed within 1 min following irradiation by a short pulse of a 375 nm laser, and was superior to that of the membrane-permeable uncaged analogue. It should be mentioned that synthesis of PI(3,4,5)P$_3$ suffered from low yield (2.5% overall) due to poor stability of the coumarylmethyl group under alkylation conditions.

Due to very fast release rates (2×10^8 s^{-1}), high photoefficiencies and hydrolytic stability, the coumarin-4-ylmethyl cage is ideal for studies of biological processes involving release of nucleotides and nucleosides. Furthermore, the intense absorptivity of 7-aminocoumarins at longer wavelengths (350–400 nm), far beyond that of other photoremovable groups, permits efficient photorelease nicely avoiding biologically lethal wavelengths. Thus, Bendig and Giese suggested 7-diethylaminocoumarin-4-ylmethyl cytidine 5′-diphosphate (CDP) **12** ($\lambda_{max} = 392$ nm; $\varepsilon = 16\,200$ M^{-1} cm^{-1}) as a suitable model for studies of a long-range radical transfer mechanism in *E. coli* ribonucleotide reductase (RNR) (Scheme 8).[57] An important advantage of this model over *o*-nitrobenzyl and other analogues is that photo-activation of CDP occurs extremely fast, which permits analysis of conformational changes preceding the radical transfer, and at wavelengths where the molar absorptivity of RNR is very low.[57]

The release of ATP in cell cultures and in acutely isolated brain slices was tested to probe the ability to evoke Ca^{2+} ion waves[53] (Scheme 9). The release of nucleoside triphosphate from caged precursor **13** in HEPES solution was twice as efficient as that of the nitrobenzyl-caged analog at 365 nm and ten times more efficient at 405 nm. To measure the response in cells, cytosolic Ca^{2+} concentrations were recorded from confluent astroglial cultures stained with the Ca^{2+} indicator fluo-3. The experiments confirmed biological inertness of the caged ATP **13**. In contrast, irradiation of the latter with an argon laser at 364 nm caused a notable increase of fluorescence in cells close to the UV spot. The response was successfully elicited

three times, provided the cells were allowed to recover after each dose of radiation. The Ca^{2+} response showed the typical time course of an ATP-triggered signal: a fast increase in cytosolic Ca^{2+} concentration and a subsequent slow decay back to the initial concentration.[53]

Light-controlled, *in vitro* enzymatic polymerization of nucleic acids through the release of ATP from a coumarin-4-ylmethyl-caged precursor was demonstrated by Baptista (Scheme 9)[54] by irradiating a ribonucleotide mixture (CTP, UTP, and GTP) and caged ATP **13**. A control sample (no light) showed no reaction, whereas formation of the transcription product was formed on irradiation, reaching a maximum at 25 μM of ATP followed by a decrease in RNA formation. The decrease in RNA was explained by inhibition of transcription due to accumulation of byproduct **15**.[54]

The release rate of the cyclic nucleotide depends on its structure and the solvent polarity.[68] High electron donor ability of the purine base compared with diethyl phosphate leads to more stable intermediate tight ion pairs resulting in greater quantum yields. Furthermore, the higher quantum yields for the axial *vs.* equatorial isomers of caged cyclic phosphates (0.13–0.21 for **16** *vs.* 0.07–0.09 for **17**, Scheme 10) were attributed to increased steric interaction and larger partial charge transfer between the purine base and coumarylmethyl cation for the axial *vs.* equatorial isomer.

The effect of substituents on coumarin PPGs was systematically investigated for a series of caged cAMPs (Scheme 11).[44] In addition to influencing the absorption maxima (Table 2), changing donor substituents at the 6- and 7-position of coumarin also significantly affects the quantum yields. The highest quantum yields are obtained for 7-dialkylamino derivatives (0.21–0.28), which were rationalized by more efficient stabilization of the coumarylmethyl carbocation through the electron-donating amino substituents and, as a result, more efficient ion pair escape (Scheme 11).[44,68]

Iwamura and coworkers were the first to probe photorelease of cAMP from a coumarin cage in studies of biological responses within living cells.[69,70] A test experiment using zebra fish melanophores demonstrated that inactive, caged cAMP (**18**, X = Br, Y = AcO, Scheme 11) successfully penetrated through the plasma membrane into the melanophore and released a sufficient amount of cAMP upon irradiation at 340–365 nm to induce motile response of melanin granules. This has been revisited for coumaryl PPGs possessing a polar aminobis(methylcarboxylate) group (**19**, Scheme 12), which significantly improved water solubility of the caged nucleoside monophosphates.[47,60] Furthermore, the fluorescence quantum yields of **19a,b** were an order of magnitude lower than that of the corresponding coumarin-4-ylmethanol **20**, which permitted convenient monitoring of the reaction by fluorescence spectroscopy. Upon irradiation of HEK293 cells transfected with DNA encoding CNGA2 channels, loaded with **19b**, an increase in both the intracellular fluorescence and the cAMP-induced current resulting from activation of olfactory neurons (CNGA2) was observed.[47] From these studies, coumarylmethyl PPGs can be used as an analytical method for quantitative dose–response relationships for cellular reactions triggered by cAMP.

In addition to significant advances achieved in caging of DNA and RNA through the phosphate backbone using methods described above, complementary approaches for base-caged nucleosides have also been developed to enable control of Watson–Crick pairing and double strand formation. Bromocoumarylmethyl-caged deoxycytidine **21** and deoxyadenosines **22** used by Furuta *et al.* proved most efficient compared to *o*-nitro-benzyl caged analogues in the release of nucleosides upon irradiation at 350 nm (Scheme 13).[49]

The coumarylmethyl chromophore has been increasingly examined for 2-photon excitation efficacy using near IR (>700 nm) lasers.[71] Thus, it was also shown that the two-photon uncaging action cross-section of **22a** (0.35 GM at 740 nm) is in the practical range for biological applications. The *O*-caged deoxyguanosines **23** reported by Heckel showed significantly lower quantum yields at 365 nm as compared to *P*-caged cyclic nucleotides or the 2-(*o*-nitrophenyl)propyl analogue **24**; however, the high extinction coefficient of **23** makes photochemical effectiveness for release nearly two-fold better than that for **24**.[72] Furthermore, uncaging of nucleobase in **23** at 405 nm proceeded 80 times faster than the corresponding *o*NE PPG in **24**, permitting wavelength-selective photorelease.

Release of carboxylate: carboxylic acids and amino acids—The photoefficiency of the 7-alkoxycoumarin-caged carboxylates, especially aliphatic acids, is generally rather poor,[65] primarily attributed to the higher pK_a of a carboxylic acid as compared with a phosphate leaving group. Thus, Schmidt *et al.* demonstrated a strong decrease of the rate constants of heterolytic cleavage, k_{cl}, with increasing pK_a of the released acid (Fig. 4, Scheme 14, Table 3).[38]

The release of 2,4-D represents a practical, agricultural application of coumarins as PPGs. The UV-Vis photochemistry of 2,4-D caged by 7-substituted coumarylmethyl protecting groups was measured in several aqueous organic solvents to explore the effects of substituents and the pH on the solubility and the conversion at different wavelengths (Scheme 15).[73] All compounds in the tested series showed rather low efficiencies; the highest quantum yield was observed for 7-hydroxy-derivative **26** (0.018 and 0.012 at 310 and 350 nm, respectively).

Similarly, a comparison of quantum yields of three GABA conjugates **25a**–**c** at different wavelengths performed by Costa *et al.* revealed rather low photoefficiency in the UV range optimal for most biological applications (350 nm) (Scheme 16).[42,68]

In contrast to poor quantum yields observed in the previous examples employing 7-alkoxycoumaryl group, photorelease of amino acids linked through the carboxylate moiety to 7-aminocoumarylmethyl chromophore was much more efficient (Scheme 17).[46,55,56,74–76] Quantum yields for caged GABA, glycine and glutamate derivatives range from 10 to 20% (Table 4).[46,56] It was proposed that the photocleavage product yield can be attenuated by ion-pair internal return of the released group in competition with escape from the solvent cage.[46] Stability of the carboxylate-caged amino acids toward hydrolysis may become an issue and thus should always be examined prior to photolysis to ensure stability of the caged compound in aqueous buffer solution. In fact, it was found that phenylalanine caged with the water-soluble bis(carboxymethyl)amino derivative (**26c**) was unstable in HEPES buffer at pH 7.2.[74] Spontaneous hydrolysis was also observed for glutamate when caged with 6-bromo-7-hydroxycoumarin-4-ylmethyl.[66]

Coumarin-caged neurotransmitters are ideal models because they can be efficiently photolyzed by visible and near UV light that is much less harmful to cells, thereby opening biological studies to both *in vivo* and *in vitro* activation of agonists and antagonists at various neurotransmitter receptors. On the other hand, the photolysis byproducts do not appear to inhibit or activate these same receptors. The experimental design in these studies vary from more sophisticated laser-flash, time-resolved procedures to the more readily available, inexpensive light sources such as Rapp flash lamps.

Hess and coworkers employed photorelease of caged GABA, glycine, and glutamate as a tool for studying the mechanism of action of neurotransmitter receptors using HEK 293 cells transfected with cDNA encoding the corresponding receptors. Flash lamp photolysis (385–

450 nm) uncaged glycine[56] and glutamate[55] from precursors **26d,e** in HEK extracellular buffer. The efficiency of photorelease was assessed by the whole-cell current evoked by the released amino acid.[55,56] Both caged glycine (**26d**) and glutamate (**26e**) were inert toward the corresponding receptors. The analogous GABA derivative **26f**, however, inhibited GABA$_A$ receptors.[75,76] This problem was addressed through the installation of an additional substituent at 4-methylene group (**26g**, X = CONHCH$_2$CO$_2$Et, Scheme 17) of the coumarin phototrigger which helped eliminate unwanted activity of the caged precursor.[76]

Carbamate-caged amino acids—To address the hydrolysis issue, amino acids caged at the N-terminus *via* a carbamate linkage were employed. Thus, carbamate-caged blockers for glutamate transporter, L-*threo*-β-benzyloxyaspartate (L-TBOA) and its more potent *m*-(trifluoromethyl)benzamide analog (L-TFB–TBOA) were found to be more stable in aqueous solutions than the corresponding carboxylates (Scheme 18).[45] Furthermore, hydrophilic coumarin-4-ylmethylcarbamate cage **27b,c** (R^2 = OCH$_2$COOH) photolyzed efficiently with quantum yields 0.03 and 0.02 (for **27b** and **27c**, respectively), which is comparable to that of the complementary carboxylate-caged analogs. Tests were conducted using **27a**–**c** on biological activity by the glutamate uptake inhibition assay using excitatory amino acid transporter (EAAT2) stably expressed on MDCK cells. It was shown that the activity of carbamate- and carboxylate-protected blockers was efficiently masked by the coumarin cage. The release of the more potent L-TFB-TBOA upon photolysis provided a sufficiently effective concentration of the blocker for applications in biological preparations. It was also confirmed by uptake assay that the blocker activity of the released L-TFB-TBOA was not impeded by the photolysis byproducts.[45]

Comparison of irradiation doses required to release amino acids caged through different linkages revealed the following relative photosensitivity order: anhydride > ester > carbamate > carbonate, with carbamates being slightly more resistant to irradiation than carboxylates (Scheme 19).[40] It should be mentioned that the rate-limiting step in all these cases except carboxylate **31** is decarboxylation of the released carbamic and carbonic acid, which depends on the nature of the released group,[77,78] and varies with pH. The rates of decarboxylation reactions are usually quite slow, $k_{-CO_2} = 10^{-3}$ s^{-1},[79–81] and subject to both acid and base catalysis.

Schmidt's calculated shifts in the λ_{max} of 7-amino-substituted coumarin-caged GABA **32** suggested a notable bathochromic shift as compared with the 7-hydroxy- and 7-methoxy derivatives.[41] Indeed, the absorption maximum of caged GABA **32** was shifted by 22–24 nm and readily released amino acid at 300–400 nm with a quantum yield of 0.04 (Scheme 20). Photolysis of caged GABA **32** on auditory neurons in the lateral superior olive in brainstem slices of mice triggered membrane current mediated by specific activation of the GABA$_A$ receptor by whole-cell patch clamp recordings of individual neurons.[41] It was shown that GABA derivative **32** had no intrinsic biological activity and good stability in dark solutions, while another caged neurotransmitter, 6-bromo-7-hydroxycoumarin-4-ylmethoxycarbonyl dopamine, was found to be more susceptible to hydrolysis in aqueous solutions, which, however, was slow enough on the timescale of the physiological experiments to allow useful studies.[51]

Applications of photoremovable groups in protein chemistry face a number of limitations, including synthetic challenges associated with chemo- and site-specific installation of PPGs, difficulty in transporting caged proteins into a cell, poor tissue penetration and damaging effects by UV light causing unwanted side reactions, such as photooxidation, and incomplete uncaging in biological environment. Often, small PPG chromophores fail to efficiently suppress the activity of large biological entities resulting in notable residual

activity.[82] Described below are several recent reports of the successful use of coumarin PPGs in caging strategies for peptides and other large biomolecules.

The coumarylmethyl cage was successfully used to mask the activity of oligopeptides Aβ1–24 and Aβ27–42 (Scheme 21).[61] An elegant approach termed "click peptide" involved an *O–N* intramolecular acyl migration triggered by cleavage of the PPG. Screening of different photoremovable groups, including 6-nitroveratryl, *p*-dimethylaminophenacyl and various 7-aminocoumarylmethyl analogs revealed that only the bis(carboxymethyl) aminocoumarylmethyl derivative possessed the necessarily important features of sufficient hydrophilicity and stability to hydrolysis. Importantly, the protected oligopeptide precursor **33** was significantly more water soluble than the target peptide Aβ1–42 (**35**), and did not self-assemble, because the *O*-acyl (instead of *N*-acyl) fragments in **33** suppressed the conformational transition into a β-sheet analogous to **35**. Irradiation of **33** at 355 nm quantitatively removed the protecting group within 2 min; subsequent incubation of **34** for 30 min at 37 °C enabled smooth acyl migration to produce **35** (Scheme 21).[61]

Another example showcasing the application of a photoremovable coumarin group in synthesis of peptidoconjugates was demonstrated by Nagamune *et al.* (Scheme 22).[83] Temporal and spatial control of peptide release was achieved upon irradiation of a peptide conjugate possessing a photocleavable backbone. Solutions of conjugates **36** and **38** possessing a bifunctional bromocoumarin carbamate linker were photolyzed at 350 nm, releasing peptides **37** and **39** with quantum yields of 0.16 and 0.26, respectively. A similar approach was employed for site-specific caging and photorelease of plasmid DNA.[84]

Coumarin-containing lipids are another example for successful use of photocleavable fragments implanted in the backbone of a complex biological molecule (Scheme 23).[52] Light-mediated release of the liposomal content *via* lipid cleavage represents an attractive alternative for controlled drug release. A hydrophilic head of the lipid (an amino acid) was separated from the hydrophobic tail by a bifunctional coumarin phototrigger carbamate link at one end and a carboxylate group at C7 as the tether (**40**). The hydrophobic head was cleaved upon irradiation, which released the amino acid from the coumarylmethyl stearate **41**. Liposomes that incorporated 20% of **40** were compared in size before and after irradiation and found to decrease in diameter by 50% as a result of the liposome reorganization and leakage.[52]

A caging strategy for masking the biological activity of a complex, heavily functionalized molecule such as Isotaxel was demonstrated by Kiso *et al.* (Scheme 24).[85] Isotaxel, an *O*-acyl isoform of the anticancer agent Paclitaxel, was modified to suppress the pharmacophore activity through caging the benzylamine moiety with a coumaryl PPG. The resulting photoresponsive prodrug, called Phototaxel (**42**), was selectively activated by visible light (430 nm) releasing Isotaxel (**43**), which in turn was converted into Paclitaxel (**44**) by a spontaneous intra-molecular *O–N*-acyl migration (Scheme 24).[85] The yield of released Paclitaxel was found to be 69%; partial loss of material was attributed to formation of unidentified side photoproducts. To improve water solubility of the Phototaxel prodrug, the *N*-ethyl groups of the coumarin cage were replaced with *N*-(2-(dimethylamino)ethyl)acetamide groups (Scheme 24).[86] *N*- and *O*-protected Paclitaxel prodrugs **45** and **46** with carbamate and carbonate-linked coumarins were synthesized. Both caged compounds showed excellent water solubility; however, carbonate **46** was not stable to aqueous solutions. Notably, direct continuous irradiation (365 nm) by a UV ray lamp released Paclitaxel from **45** very effectively, whereas pulsed laser activation (355 nm) resulted in substantial decomposition.[86]

Effective release by irradiation at long wavelengths and excellent quantum yields for the 7-aminocoumarin derivatives make them the protecting group of choice *vis-à-vis* other PPGs for wavelength-selective uncaging.[87,88] Thus, del Campo *et al.* used a pair of wavelength-based nearly orthogonal photoactivated protecting groups, a 7-diethylaminocoumarin (λ_{max} = 390–400 nm) and a nitroveratryloxycarbonyl (λ_{max} = 356 nm), each individually attached through an amino group tethered to a silica surface (Scheme 25).[87] Sequential spatially controlled wavelength exposures, first with 412 nm and then 345 nm light, selectively deprotected coumarin and nitroveratryloxycarbonyl groups creating patterns which were visualized by *in situ* subsequent coupling of the uncaged amino groups with different fluorescent dyes. Reversing the exposure sequence to first 345 nm light followed by 412 nm resulted in simultaneous cleavage of both chromophores at 345 nm due to the overlap and similar extinction coefficients of both PPGs at this wavelength.

The study further expanded the controllable variables from spatial and time-resolution to include wavelength selectivity by employing a variety of caging groups that are activated over a range of excitation wavelengths. A clear objective of this study was to identify truly orthogonal chromophores for activation of functional groups, an objective of many synthetic applications in protecting group chemistry. Seven caging chromophores, ranging from *p*HP (λ_{max} 270 nm) to coumaryl (λ_{max} 350 nm), were attached to a carboxylate group poised on an alkyl tether bound to a glass surface by a $Si(OMe)_3$ linkage. Systematic variation of the exposure wavelength to the coated silica plate released the functional carboxylate groups. The chromophores gave an effective wavelength range between 250 and 450 nm. Analysis of the seven chromophores further demonstrated that pairwise, triplet and quartet sets of orthogonal protecting groups from the variety of caging chromophore combinations could be generated on a single platform. This approach holds promise for new applications of sensors that offer more precise control for molecular detection and for communication purposes.

A photoremovable coumarin protection was employed by Wylie and Shoichet in a clever design of three-dimensional pattern-writing medium (Scheme 26).[89] The matrix, composed of modified aragose **47** possessing an exposed amino group protected with 6-bromo-7-hydroxycoumarin, was chosen for its high efficiency in two-photon activation. Confocal microscopy using a Ti-sapphire laser for 3D multiphoton uncaging cleaved the coumarin protecting group liberating the primary amine moieties in the gel.

Thiols—Analogously, unmasking sulfide groups upon UV light exposure in thiolated aragose gels **48** provided a convenient, chemospecific 3D pattern at the reaction site in preparation for selective immobilization of biologically relevant substrates (Scheme 26).[90] This approach preserves the mechanical properties of the patterned material, enabling the creation of complex 3D biochemical sites buried within hydrogels.[89,90]

Photolabile coumarin thiocarbonate protecting groups for thiols were developed by Hagen *et al.*[48,74] Two complementary PPGs, 7-aminocoumarin **49** (λ_{max} 450 nm) and 7,8-biscarboxy-methoxycoumarin **50** (λ_{max} 324 nm), were employed to mask two different cysteine residues in resact, a sea urchin peptide hormone guanylate cyclase plasma membrane (Scheme 27).[48] Notably, both PPGs were stable to TFA, which makes them orthogonal to many conventional peptide protecting groups. Irradiation of the protected resact with 402 nm light led to selective cleavage of **49**, releasing **50**-OH and two resact isomers, the result of an S-to-S acyl shift of the remaining **50** group, thereby freeing a Cys^1 side chain. Subsequent irradiation of the product mixture at 325 nm quantitatively removed **50** from the peptide. Although careful tuning of substituents on the PPG allowed clean wavelength-selective photochemistry, the observed acyl migration within resact rendered thiocarbonate PPGs inappropriate for selective protection of cysteine residues in a peptide.[48]

Alcohols and phenols—Furuta *et al.* compared several carbonate-tethered coumarin phototriggers for their efficient release of alcohols (Scheme 28).[43] All coumarin PPGs tested were found to be at least an order of magnitude more efficient than *o*-nitrobenzyl. Within the coumarins, the 7-methoxy- and 6-bromo-7-hydroxy-analogs **51a** and **51b** provided the highest quantum yields, and **51b** was the most efficient among all the tested cages. A few biologically relevant alcohols caged with **51b** showed moderate to good resistance to hydrolysis, and all caged compounds efficiently released substrates upon photolysis at 350 nm.[43]

Alkylation of the phenolic moiety of rosamine (**52**) with coumarin-4-ylmethyl chloride followed by base-promoted spirocyclization destroyed conjugation in the xanthene ring and completely shut off the fluorescence of **53** (Scheme 29).[91] Brief exposure of **53** to visible light induced a large fluorescence enhancement typical for rosamine dye (577 nm), indicating efficient probe release and restored conjugation in xanthene. Notably, the fluorescence spike in this case was much more pronounced indicating very efficient photorelease, when compared with release of rhodamine from the *o*-nitrobenzyl cage.[92]

Caged capsaicin **54**, possessing the {7-[bis(carboxymethyl) amino]coumarin-4-yl}methoxycarbonyl PPG, was employed to study capsaicin's effect on HEK 293 cells transfected with TRPV1 channels – cation channels that mediate pain perception in nociceptive somatosensory neurons (Scheme 30).[93] Preliminary tests showed that carbonate **54** had no residual activity at the micromolar level, was sufficiently resistant to hydrolysis in the dark, and efficiently released capsaicin **55** at 365 or 405 nm.[51,93] Isothermal titration calorimetry showed that the modified capsaicin **54** did not measurably translocate across a phospholipid membrane and thus can be selectively applied to one side of the plasma membrane. The effect of intracellular and extracellular photorelease of capsaicin from membrane-impermeant **54** was investigated. It was found that extracellular release of **55** triggered large whole-cell current and strong desensitization, whereas the analogous response was rather modest from intracellular release of capsaicin.[93]

Carbonyl compounds—The first example of utilizing photo activation of coumarylmethyl-caged carbonyl compounds in a biological system was reported by Hagen *et al.* (Scheme 31).[94] The rate of the primary reaction (**56** → **57**) was found to be $(1.2 \pm 0.5) \times 10^8 \ s^{-1}$ and the yield of progesterone (**57**) release was about 30%. The quantum yield was low but acceptable for the application, due to high absorptivities that ensure high photosensitivity. Caged **56** was also sensitive to 2PE; exposure of **56** to femtosecond pulses at 755 nm caused significant release of progesterone. However, the efficiency was *ca.* 5 times lower than that observed for an analogous glutamate derivative.[66]

Conclusions

The coumarylmethyl and *p*HP photoremovable protecting groups are being developed as photoinitiators for mechanistic studies in biological transformations that require nanosecond release rates. They are synthetically accessible and can be installed readily on most substrates. Recent advances in time resolved spectroscopy encourage yet further development of these new PPGs.

Acknowledgments

Notes and references

1. (a) Pelliccioli AP, Wirz J. Photoremovable protecting groups: reaction mechanisms and applications. Photochem Photobiol Sci. 2002; 1:441. [PubMed: 12659154] (b) Bochet CG. Photolabile protecting groups and linkers. J Chem Soc, Perkin Trans. 2002; 1:125.(c) Goeldner, M.; Givens, R., editors. Dynamic Studies in Biology: Phototriggers, Photoswitches and Caged Biomolecules. Wiley-VCH; Weinheim: 2005.

2. (a) Il'ichev YV, Schwörer MA, Wirz J. Photochemical reaction mechanisms of 2-nitrobenzyl compounds: methyl ethers and caged ATP. J Am Chem Soc. 2004; 126:4581. [PubMed: 15070376] (b) Hellrung B, Kamdzhilov Y, Schwörer M, Wirz J. Photorelease of alcohols from 2-nitrobenzyl ethers proceeds via hemiacetals and may be further retarded by buffers intercepting the primary aci-nitro intermediates. J Am Chem Soc. 2005; 127:8934. [PubMed: 15969554]

3. Du X, Frei H, Kim S-H. Comparison of nitrophenylethyl and hydroxyphenacyl caging groups. Biopolymers. 2001; 62:147. [PubMed: 11343283]

4. Kötting C, Güldenhaupt J, Gerwert K. Time-resolved FTIR spectroscopy for monitoring protein dynamics exemplified by functional studies of as protein bound to a lipid bilayer. Chem Phys. 201110.1016/j.chemphys.2011.08.007

5. (a) Givens RS, Park CH. p-Hydroxyphenacyl ATP: a new photo-trigger. Tetrahedron Lett. 1996; 37:6259.(b) Park CH, Givens RS. New photoactivated protecting groups. 6. p-Hydroxyphenacyl: a phototrigger for chemical and biochemical probes. J Am Chem Soc. 1997; 119:2453.

6. Givens RS, Matuszewski B. Photochemistry of phosphate esters: an efficient method for the generation of electrophiles. J Am Chem Soc. 1984; 106:6860.

7. Anderson JC, Reese CB. A photo-induced rearrangement involving aryl participation. Tetrahedron Lett. 1962; 3:1.

8. Givens RS, Heger D, Hellrung B, Kamdzhilov Y, Mac M, Conrad PG, Lee E, Cope JI, Mata-Segreda JF, Schowen RL, Wirz J. The photo-Favorskii reaction of p-hydroxyphenacyl compounds is initiated by water-assisted, adiabatic extrusion of a triplet biradical. J Am Chem Soc. 2008; 130:3307. [PubMed: 18290649]

9. Pickens CJ, Gee KR. Photolabile thymidine cleavable with a 532 nanometer laser. Tetrahedron Lett. 2011; 52:4989.

10. Ma C, Kwok WM, Chan WS, Du Y, Kan JTW, Toy PH, Phillips DL. Ultrafast time-resolved transient absorption and resonance Raman spectroscopy study of the photodeprotection and rearrangement reactions of p-hydroxyphenacyl caged phosphates. J Am Chem Soc. 2006; 128:2558. [PubMed: 16492039]

11. Heger D, Wirz J. unpublished results.

12. Remes M, Roithova J, Schroeder D, Cope ED, Perera C, Senadheera SN, Stensrud K, Ma C-C, Givens RS. Gas-phase fragmentation of deprotonated p-hydroxyphenacyl derivatives. J Org Chem. 2011; 76:2180. [PubMed: 21384805]

13. For quantum yields, see ref. 5, 8, 10 and 15, and Cope E. PhD thesis. University of Kansas2007

14. Zhang K, Corrie JET, Munasinghe VRN, Wan P. Mechanism of photosolvolytic rearrangement of p-hydroxyphenacyl esters: evidence for excited-state intramolecular proton transfer as the primary photochemical step. J Am Chem Soc. 1999; 121:5625.We have also tested our pHP derivatives for stability in base (pH > 9) in control experiments and found no rearrangement products.

15. (a) Givens, RS.; Weber, JFW.; Jung, AH.; Park, C-H. New photo-protecting groups: desyl and p-hydroxyphenacyl phosphate and carboxylate esters. In: Marriott, G., editor. Methods in Enzymology. Vol. 291. Academic Press; New York: 1998. p. 1(b) Givens RS, Yousef AL. p-Hydroxyphenacyl: a photoremovable protecting group for caging bio-active substrates. :55. ref. 1c.

16. See: Givens RS, Weber JFW, Conrad PG II, Orosz G, Donahue SL, Thayer SA. New phototriggers 9: p-hydroxyphenacyl as a C-terminal photoremovable protecting group for oligopeptides. J Am Chem Soc. 2000; 122:2687.Conrad PG II, Givens RS, Weber JF, Kandler K. New phototriggers:1 extending the p-hydroxyphenacyl π–π* absorption range. Org Lett. 2000; 2:1545. [PubMed: 10841475] for early examples of amino acid neurotransmitter and oligopeptide applications

17. Givens RS, Stensrud K, Conrad PG II, Yousef AL, Perera C, Senadheera SN, Heger D, Wirz J. p-Hydroxyphenacyl photoremovable protecting groups: robust photochemistry despite substituent diversity. Can J Chem. 2011; 89:364.

18. Conrad PG II, Givens RS, Hellrung B, Rajesh CS, Ramseier M, Wirz J. p-Hydroxyphenacyl phototriggers: the reactive excited state of phosphate photorelease. J Am Chem Soc. 2000; 122:9346.

19. Givens, RS.; Conrad, PG., II; Yousef, AL.; Lee, J-I. Photoremovable protecting groups. In: Horspool, WM., editor. CRC Handbook of Organic Photochemistry and Photobiology. 2. Vol. ch 69. 2003.

20. Givens RS, Lee J-I. The p-hydroxyphenacyl photoremovable protecting group. J Photoscience. 2003; 10:37.

21. Kötting C, Surveyzdis Y, Bojja RS, Metzler-Nolte N, Gerwert K. Label-free screening of drug–protein interactions by trFTIR spectroscopic assays exemplified by Ras interactions. Appl Spectrosc. 2010; 64:967. [PubMed: 20828432]

22. (a) Ma C, Kwok WM, Chan WS, Zuo P, Kan JTW, Toy PH, Phillips DL. Ultrafast time-resolved study of photophysical processes involved in the photodeprotection of p-hydroxyphenacyl caged phototrigger compounds. J Am Chem Soc. 2005; 127:1463. [PubMed: 15686379] (b) Chen X, Ma C, Kwok WM, Guan X, Du Y, Phillips DL. A theoretical investigation of p-hydroxyphenacyl caged phototrigger compounds: an examination of the excited state photochemistry of p-hydroxyphenacyl acetate. J Phys Chem A. 2006; 110:12406. [PubMed: 17091942] (c) Ma C, Chan WS, Kwok WM, Zuo P, Phillips DL. Time-resolved resonance Raman study of the triplet state of the p-hydroxyphenacyl acetate model phototrigger compound. J Phys Chem B. 2004; 108:9264.(d) Ma C, Zuo P, Kwok WM, Chan WS, Kan JTW, Toy PH, Phillips DL. Time-resolved resonance Raman study of the triplet states of p-hydroxyacetophenone and the p-hydroxyphenacyl diethyl phosphate phototrigger compound. J Org Chem. 2004; 69:6641. [PubMed: 15387586]

23. Chen X, Ma C, Kwok WM, Guan X, Du Y, Phillips DL. A theoretical investigation of p-hydroxyphenacyl caged phototrigger compounds: how water induces the photodeprotection and subsequent rearrangement reactions. J Phys Chem B. 2007; 111:11832. [PubMed: 17867669]

24. Geibel S, Barth A, Amslinger S, Jung AH, Burzik C, Clarke RJ, Givens RS, Fendler K. P3-[2-(4-hydroxyphenyl)-2-oxo]ethyl ATP for the rapid activation of the Na$^+$, K$^+$-ATPase. Biophys J. 2000; 79:1346. [PubMed: 10968997]

25. Specht A, Loudwig S, Peng L, Goeldner M. p-Hydroxyphenacyl bromide as photoreversible thiol label: a potential phototrigger for thiol-containing biomolecules. Tetrahedron Lett. 2002; 43:8947.

26. (a) Zou K, Miller WT, Givens RS, Bayley H. Caged thiophosphotyrosine peptides. Angew Chem, Int Ed. 2001; 40:3049.(b) Zou K, Cheley S, Givens RS, Bayley H. Catalytic subunit of protein kinase A caged at the activating phosphothreonine. J Am Chem Soc. 2002; 124:8220. [PubMed: 12105899]

27. Du X, Frei H, Kim S-H. The mechanism of GTP hydrolysis by Ras probed by Fourier transform infrared spectroscopy. J Biol Chem. 2000; 275:8492. [PubMed: 10722686]

28. Kötting C, Gerwert K. Time-resolved FTIR studies provide activation free energy, activation enthalpy and activation entropy for GTPase reactions. Chem Phys. 2004; 307:227.

29. Sot B, Kötting C, Deaconescu D, Suveyzdis Y, Gerwert K, Wittinghofer A. Unravelling the mechanism of dual-specificity GAPs. EMBO J. 2010; 29:1205. [PubMed: 20186121]

30. Conrad, PGC.; Chavli, RV.; Givens, RS. Caged substrates applied to high content screening: an introduction with an eye to the future. In: Giuliano, KA.; Haskins, J.; Taylor, DL., editors. High Content Screening: A Powerful Approach in Systems Cell Biology and Drug Discovery, Methods in Molecular Biology. Humana Press Inc; Totowa, NJ, United States: 2007. p. 253

31. (a) Kötting C, Kallenbach A, Suveyzdis Y, Eichholz C, Gerwert K. Surface change of Ras enabling effector binding monitored in real time at atomic resolution. ChemBioChem. 2007; 8:781. [PubMed: 17385754] (b) Warscheid B, Brucker S, Kallenbach A, Meyer HE, Gerwert K, Kötting C. Systematic approach to group-specific isotopic labeling of proteins for vibrational spectroscopy. Vib Spectrosc. 2008; 48:28.

32. Brucker S, Gerwert K, Kötting C. Try 39 of ran preserves the Ran. GTP gradientby inhibiting GTP hydrolysis. J Mol Biol. 2010; 401:1–6. [PubMed: 20609434]

33. Arabaci G, Guo X-C, Beebe KD, Coggeshall KM, Pei D. r-Haloacetophenone derivatives as photoreversible covalent inhibitors of protein tyrosine phosphatases. J Am Chem Soc. 1999; 121:5085.

34. Greene, TW.; Wutts, PGM. Greene's Protective Groups in Organic Synthesis. 4. Wiley-Interscience, J. Wiley and Sons; 2007.

35. Alvarez M, Alonso JM, Filevich O, Bhagawati M, Etchenique R, Piehler J, del Campo A. Modulating surface density of proteins via caged surfaces and controlled light exposure. Langmuir. 2011; 27:2789.

36. Ellis-Davies GCR. Caged compounds: photorelease technology for control of cellular chemistry and physiology. Nat Methods. 2007; 4:619. [PubMed: 17664946] Dorman KG, Prestwich GD. Using photolabile ligands in drug discovery and development. Trends Biotechnol. 2000; 18:54.Kikuchi Y, Nakanishi J, Shimizu T, Nakayama H, Inoue S, Yamaguchi K, Iwai H, Yoshida Y, Horiike Y, Takarada T, Maeda M. Arraying heterotypic single cells on photoactivatable cell-culturing substrates. Langmuir. 2008; 24:13084. [PubMed: 18925763] and references therein; Pirrung MC, Rana VS. Photoremovable protecting groups in DNA synthesis and microarray fabrication. :341. ref. 1c.

37. See, for example: (Casey JP, Blidner RA, Monroe WT. Caged siRNAs for spatiotemporal control of gene silencing. Mol Pharmacol. 2009; 6:669.Lee H-M, Larson DR, Lawrence DS. Illuminating the chemistry of life: design, synthesis, and applications of "caged" and related photoresponsive compounds. ACS Chem Biol. 2009; 4:409. [PubMed: 19298086] Mayer G, Heckel A. Biologically active molecules with a "light switch". Angew Chem, Int Ed. 2006; 45:4900.Young DD, Deiters A. Photochemical control of biological processes. Org Biomol Chem. 2007; 5:999. [PubMed: 17377650]

38. Schmidt R, Geissler D, Hagen V, Bendig J. Mechanism of photo-cleavage of (coumarin-4-yl)methyl esters. J Phys Chem A. 2007; 111:5768. [PubMed: 17564421]

39. Schultz C. Molecular tools for cell and systems biology. HFSP J. 2007; 1:230. [PubMed: 19404424]

40. Fonseca ASC, Gonçalves MST, Costa SPG. Photocleavage studies of fluorescent amino acid conjugates bearing different types of linkages. Tetrahedron. 2007; 63:1353.

41. Cürten B, Kullmann PHM, Bier ME, Kandler K, Schmidt BF. Synthesis, photophysical, photochemical and biological properties of caged GABA, 4-[[(2H-1-benzopyran-2-one-7-amino-4-methoxy) carbonyl] amino] butanoic acid. Photochem Photobiol. 2005; 81:641. [PubMed: 15623351]

42. Fernandes MJG, Gonçalves MST, Costa SPG. Comparative study of polyaromatic and polyheteroaromatic fluorescent photocleavable protecting groups. Tetrahedron. 2008; 64:3032.

43. Suzuki AZ, Watanabe T, Kawamoto M, Nishiyama K, Yamashita H, Ishii M, Iwamura M, Furuta T. Coumarin-4-ylmethoxycarbonyls as phototriggers for alcohols and phenols. Org Lett. 2003; 5:4867. [PubMed: 14653694]

44. Eckardt T, Hagen V, Schade B, Schmidt R, Schweitzer C, Bendig J. Deactivation behavior and excited-state properties of (coumarin-4-yl)methyl derivatives. 2. Photocleavage of selected (coumarin-4-yl)methyl-caged adenosine cyclic 3′,5′-monophosphates with Fluorescence enhancement. J Org Chem. 2002; 67:703. [PubMed: 11856009]

45. Takaoka K, Tatsu Y, Yumoto N, Nakajima T, Shimamoto K. Synthesis of carbamate-type caged derivatives of a novel glutamate transporter blocker. Bioorg Med Chem Lett. 2004; 12:3687.

46. Senda N, Momotake A, Arai T. Synthesis and photocleavage of 7-[{bis(carboxymethyl)amino}coumarin-4-yl]methyl-caged neurotransmitters. Bull Chem Soc Jpn. 2007; 80:2384.

47. Hagen V, Frings S, Bendig J, Lorenz D, Wiesner B, Kaupp UB. Fluorescence spectroscopic quantification of the release of cyclic nucleotides from photocleavable [bis(carboxymethoxy)coumarin-4-yl]methyl esters inside cells. Angew Chem, Int Ed. 2002; 41:3625.

48. Kotzur N, Briand B, Beyermann M, Hagen V. Wavelength-selective photoactivatable protecting groups for thiols. J Am Chem Soc. 2009; 131:16927. [PubMed: 19863095]

49. Furuta T, Watanabe T, Tanabe S, Sakyo J, Matsuba C. Phototriggers for nucleobases with improved photochemical properties. Org Lett. 2007; 9:4717. [PubMed: 17929824]

50. Lu M, Fedoryak OD, Moister BR, Dore TM. Bhc-diol as a photolabile protecting group for aldehydes and ketones. Org Lett. 2003; 5:2119. [PubMed: 12790543]

51. Hagen V, Kilic F, Schaal J, Dekowski B, Schmidt R, Kotzur N. [8-[Bis(carboxymethyl)aminomethyl]-6-bromo-7-hydroxycoumarin-4-yl] methyl moieties as photoremovable protecting groups for compounds with COOH, NH2, OH, and C=O functions. J Org Chem. 2010; 75:2790. [PubMed: 20356068]

52. Subramaniam R, Xiao Y, Li Y, Qian SY, Sun W, Mallik S. Light-mediated and H-bond facilitated liposomal release: the role of lipid head groups in release efficiency. Tetrahedron Lett. 2010; 51:529.

53. Geissler D, Kresse W, Wiesner B, Bendig J, Kettenmann H, Hagen V. DMACM-caged adenosine nucleotides: ultrafast phototriggers for ATP, ADP and AMP activated by long-wavelength irradiation. Chem-BioChem. 2003; 4:162.

54. Pinheiro AV, Baptista P, Lima JC. Light activation of transcription: photocaging of nucleotides for control over RNA polymerization. Nucleic Acids Res. 2008; 36:e90. [PubMed: 18586819]

55. Shembekar VR, Chen Y, Carpenter BK, Hess GP. A protecting group for carboxylic acids that can be photolysed by visible light. Biochemistry. 2005; 44:7107. [PubMed: 15882049]

56. Shembekar VR, Chen Y, Carpenter BK, Hess GP. Coumarin-caged glycine that can be photolyzed within 3 microseconds by visible light. Biochemistry. 2007; 46:5479. [PubMed: 17425336]

57. Schönleber RO, Bendig J, Hagen V, Giese B. Rapid photolytic release of cytidine 5′-diphosphate from a coumarin derivative: a new tool for the investigation of ribonucleotide reductases. Bioorg Med Chem. 2002; 10:97. [PubMed: 11738611]

58. Skwarczynski M, Noguchi M, Hirota S, Sohma Y, Kimura T, Hayashi Y, Kiso Y. Development of first photoresponsive prodrug of paclitaxel. Bioorg Med Chem Lett. 2006; 16:4492. [PubMed: 16806915]

59. Senda N, Momotake A, Arai T. Synthesis and photocleavage of 7-[{bis(carboxymethyl)amino}coumarin-4-yl]methyl-caged neurotransmitters. Bull Chem Soc Jpn. 2007; 80:2384.

60. Hagen V, Dekowski B, Nache V, Schmidt R, Geißler D, Lorenz D, Eichhorst J, Keller S, Kaneko H, Benndorf K, Wiesner B. Coumarinylmethyl esters for ultrafast release of high concentrations of cyclic nucleotides upon one- and two-photon photolysis. Angew Chem, Int Ed. 2005; 44:7887.

61. Taniguchi A, Skwarczynski M, Sohma Y, Okada T, Ikeda K, Prakash H, Mukai H, Hayashi Y, Kimura T, Hirota S, Matsuzaki K, Kiso Y. Controlled production of amyloid β peptide from a phototriggered, water-soluble precursor "click peptide". ChemBioChem. 2008; 9:3055. [PubMed: 19025862]

62. Piloto AM, Rovira D, Costa SPG, Gonçalves MST. Oxobenzo[f]benzopyrans as new fluorescent photolabile protecting groups for the carboxylic function. Tetrahedron. 2006; 62:11955.

63. Fernandes MJG, Gonçalves MST, Costa SPG. Neurotransmitter amino acid – oxobenzo[f]benzopyran conjugates: synthesis and photorelease studies. Tetrahedron. 2008; 64:11175.

64. Pinheiro AV, Parola AJ, Baptista PV, Lima JC. pH effect on the photochemistry of 4-methylcoumarin phosphate esters: caged-phosphate case study. J Phys Chem A. 2010; 114:12795. [PubMed: 21087059]

65. Furuta T. Coumarin-4-ylmethyl phototriggers. :29. ref. 1c.

66. Kawakami T, Cheng H, Hashiro S, Nomura Y, Tsukiji S, Furuta T, Nagamune T. A caged phosphopeptide-based approach for photochemical activation of kinases in living cells. ChemBioChem. 2008; 9:1583. [PubMed: 18481344]

67. Mentel M, Laketa V, Subramanian D, Gillandt H, Schultz C. Photoactivatable and cell-membrane-permeable phosphatidylinositol 3,4,5-trisphosphate. Angew Chem, Int Ed. 2011; 50:3811.

68. Schade B, Hagen V, Schmidt R, Herbrich R, Krause E, Eckardt T, Bendig J. Deactivation Behavior and excited-state properties of (coumarin-4-yl)methyl derivatives. 1. Photocleavage of (7-methoxycoumarin-4-yl)methyl-caged acids with Fluorescence enhancement. J Org Chem. 1999; 64:9109.

69. Furuta T, Torigai H, Sugimoto M, Iwamura M. Photochemical properties of new photolabile cAMP derivatives in a physiological saline solution. J Org Chem. 1995; 60:3953.

70. Furuta T, Takeuchi H, Isozaki M, Takahashi Y, Kanehara M, Sugimoto M, Watanabe T, Noguchi K, Dore TM, Kurahashi T, Iwamura M, Tsien RY. Bhc-cNMPs as either water-soluble or membrane-permeant photo-releasable cyclic nucleotides for both one and two-photon excitation. ChemBioChem. 2004; 5:1119. [PubMed: 15300837]

71. Warther D, Gug S, Specht A, Bolze F, Nicoud J-F, Mourot A, Goeldner M. Two-photon uncaging: new prospects in neuroscience and cellular biology. Bioorg Med Chem. 2010; 18:7753. [PubMed: 20554207]

72. Menge C, Heckel A. Coumarin-caged dG for improved wavelength-selective uncaging of DNA. Org Lett. 2011; 13:4620. [PubMed: 21834506]

73. Atta S, Jana A, Ananthakirshnan R, Dhuleep PSN. Fluorescent caged compounds of 2,4-dichlorophenoxyacetic acid (2,4-D): photo-release technology for controlled release of 2,4-D. J Agric Food Chem. 2010; 58:11844. [PubMed: 20973537]

74. Hagen V, Dekowski B, Kotzur N, Lechler R, Wiesner B, Briand B, Beyermann M. {7-[bis(carboxymethyl)amino]coumarin-4-yl}methoxycarbonyl derivatives for photorelease of carboxylic acids, alcohols/ phenols, thioalcohols/thiophenols, and amines. Chem–Eur J. 2008; 14:1621. [PubMed: 18046693]

75. Shembekar VR, Carpenter BK, Ramachandran L, Hess GP. Development of photolabile protecting groups that rapidly release bio-active compounds on photolysis with visible light. Polym Prepr. 2004; 45:8893.

76. Fan L, Lewis RW, Hess GP, Ganem B. A new synthesis of caged GABA compounds for studying GABAA receptors. Bioorg Med Chem Lett. 2009; 19:3932. [PubMed: 19364648]

77. Johnson SL, Morrison DL. Kinetics and mechanism of decarboxylation of N-arylcarbamates. Evidence for kinetically important zwitterionic carbamic acid species of short lifetime. J Am Chem Soc. 1972; 94:1323. [PubMed: 5060276]

78. Papageorgiou G, Barth A, Corrie JET. Flash photolytic release of alcohols from photolabile carbamates or carbonates is rate-limited by decarboxylation of the photoproduct. Photochem Photobiol Sci. 2005; 4:216. [PubMed: 15696240]

79. Rossi FM, Kao JPY. Nmoc-DBHQ: A new caged molecule for modulating sarcoplasmic/endoplasmic reticulum Ca^{2+} ATPase activity with light flashes. J Biol Chem. 1997; 272:3266. [PubMed: 9013564]

80. Pocker Y, Davison BL, Deits TL. Decarboxylation of monosubstituted derivatives of carbonic acid. Comparative studies of water- and acid-catalyzed decarboxylation of sodium alkyl carbonates in water and water-d_2. J Am Chem Soc. 1978; 100:3564.

81. Rossi FM, Margulis M, Tang C-M, Kao JPY. N-Nmoc-glutamate: A new caged glutamate with high chemical stability and low pre-photolysis activity. J Biol Chem. 1997; 272:32933. [PubMed: 9407072]

82. Loudwig S, Bayley H. Light-activated proteins: an overview. :253–304. ref. 1c.

83. Katayama K, Tsukiji S, Furuta T, Nagamune T. A bromocoumarin-based linker for synthesis of photocleavable peptidoconjugates with high photosensitivity. Chem Commun. 2008:5399.

84. Yamaguchi S, Chen Y, Nakajima S, Furuta T, Nagamune T. Light-activated gene expression from site-specific caged DNA with a biotinylated photolabile protection group. Chem Commun. 2010; 46:2244.

85. Skwarczynski M, Noguchi M, Hirota S, Sohma Y, Kimura T, Hayashi Y, Kiso Y. Development of first photoresponsive prodrug of paclitaxel. Bioorg Med Chem Lett. 2006; 16:4492. [PubMed: 16806915]

86. Noguchi M, Skwarczynski M, Prakash H, Hirota S, Kimura T, Hayashi Y, Kiso Y. Development of novel water-soluble photocleavable protective group and its application for design of photoresponsive paclitaxel prodrugs. Bioorg Med Chem. 2008; 16:5389. [PubMed: 18440235]

87. San Miguel V, Bochet CG, del Campo A. Wavelength-selective caged surfaces: how many functional levels are possible? J Am Chem Soc. 2011; 133:5380. [PubMed: 21413802]

88. Stegmaier P, Alonso JM, del Campo A. Photoresponsive surfaces with two independent wavelength-selective functional levels. Langmuir. 2008; 24:11872. [PubMed: 18817427]

89. Wylie RG, Shoichet MS. Two-photon micropatterning of amines within an agarose hydrogel. J Mater Chem. 2008; 18:2716.

90. Woznick JH, Shoichet MS. Three-dimensional chemical patterning of transparent hydrogels. Chem Mater. 2008; 20:55.

91. Lin W, Long L, Tan W, Chen B, Yuan L. Coumarin-caged rosamine probes based on a unique intramolecular carbon–carbon spirocyclization. Chem–Eur J. 2010; 16:3914. [PubMed: 20222098]

92. Ottl J, Gabriel D, Marriott G. Preparation and photoactivation of caged fluorophores and caged proteins using a new class of heterobifunctional, photocleavable cross-linking reagents. Bioconjugate Chem. 1998; 9:143.

93. Gilbert D, Funk K, Dekowski B, Lechler R, Keller S, Möhrlen F, Frings S, Hagen V. Caged capsaicins: new tools for the examination of TRPV1 channels in somatosensory neurons. ChemBioChem. 2007; 8:89. [PubMed: 17154194]

94. Kilic F, Kashikar ND, Schmidt R, Alvarez L, Dai L, Weyand I, Wiesner B, Goodwin N, Hagen V, Kaupp UB. Caged progesterone: a new tool for studying rapid nongenomic actions of progesterone. J Am Chem Soc. 2009; 131:4027. [PubMed: 19256499]

Biographies

Richard S. Givens (1940) is an Emeritus Professor (2010) of Chemistry at the University of Kansas. He earned his BA (Chemistry, H-G. Gilde) from Marietta College and PhD (H. E. Zimmerman) from the University of Wisconsin in 1966. He was an NIH postdoctoral associate (G. A. Russell) at Iowa State. He has authored or coauthored more than 120 scientific publications and 5 patents on physical organic chemistry, photochemistry, and their applications in biology and is co-editor of *Dynamic Studies in Biology: Phototriggers, Photoswitches and Caged Biomolecules* (Wiley-VCH, 2005).

Marina Rubina received her BS degree in chemistry and chemical education from Syktyvkar State University (Russia) in 1996. She was a research associate at the Moscow State University (Russia) before earning her PhD degree with Vladimir Gevorgyan (2004) at the University of Illinois at Chicago. She was then a postdoctoral associate with Michael Rubin and Richard Givens at the University of Kansas. Currently, she is Laboratory Director in the Department of Chemistry and a Research Associate at the Center for Environmentally Beneficial Catalysis at the University of Kansas.

Jakob Wirz (1942) is Emeritus Professor of Chemistry. He studied at the ETH Zürich with Prof. E. Heilbronner and, after postdoctoral studies in London with Professors G. Porter and D. Barton, habilitated at the University of Basel, where he led a research group until 2007. He co-authored the book *Photochemistry of Organic Compounds* (Wiley, 2009) with Professor P. Klán and published over 170 papers focusing on photochemistry and spectroscopy, laser flash photolysis, reaction mechanisms, and photochemical protecting groups. He continues to serve as Deputy editor-in-chief for *Photochemical & Photobiological Sciences*.
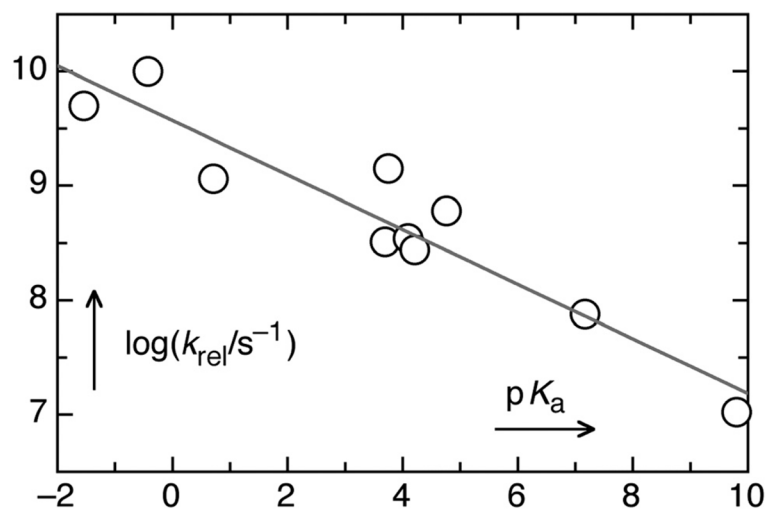
Fig. 1.
Linear free energy relationship showing the dependence of the release rate constants k_{rel} on the pK_a of the leaving group.
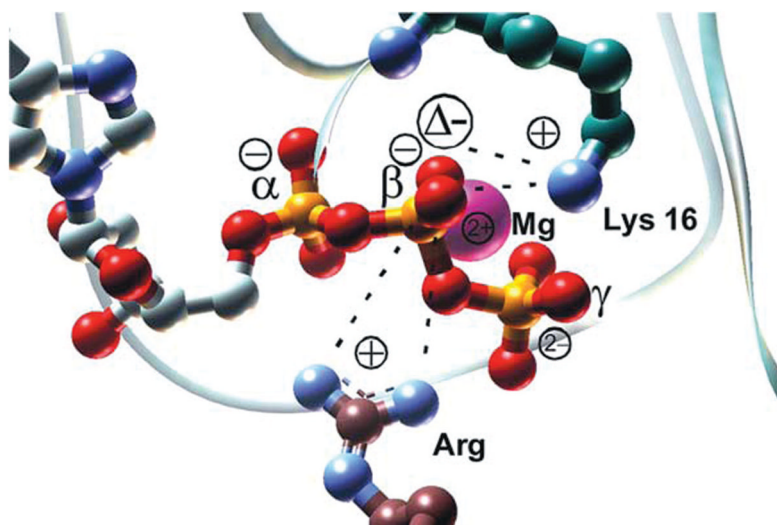
Fig. 2.
Mg^{2+} and Lys16 from Ras and the arginine finger from GAP draw negative charge towards the β-phosphate of GTP. The main catalytic effect of Ras and GAP is enthalpic and seems to originate from these electrostatic interactions. (Reprinted with permission by *Chemical Physics* (2004).[28])
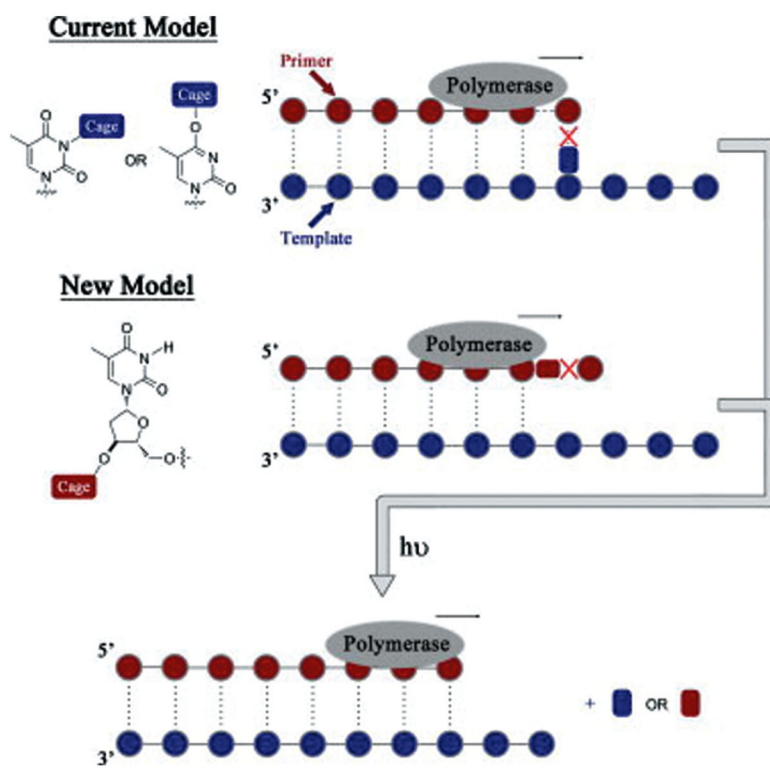
Fig. 3.
Caging methodologies to regulate oligo synthesis. (With permission of *Tetrahedron Lett.*)
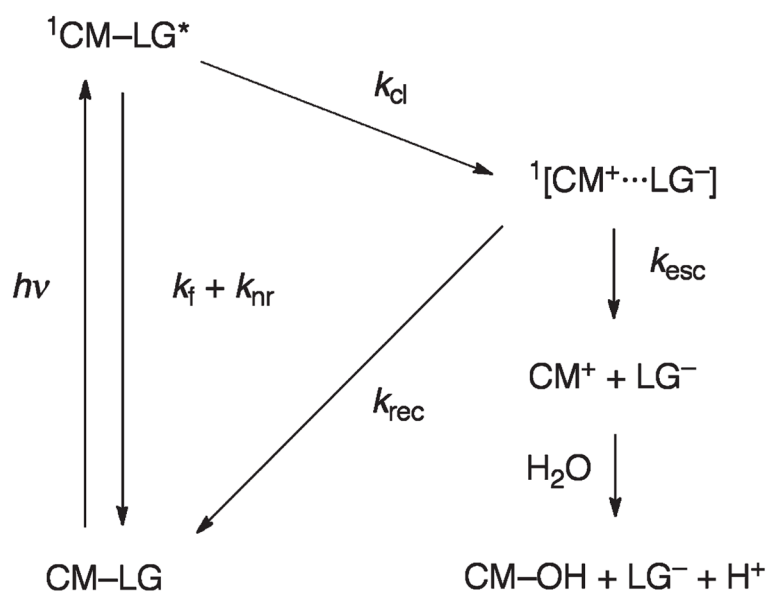
Fig. 4.
Mechanism of the photocleavage of coumarylmethyl cages. Adapted from ref. 38.
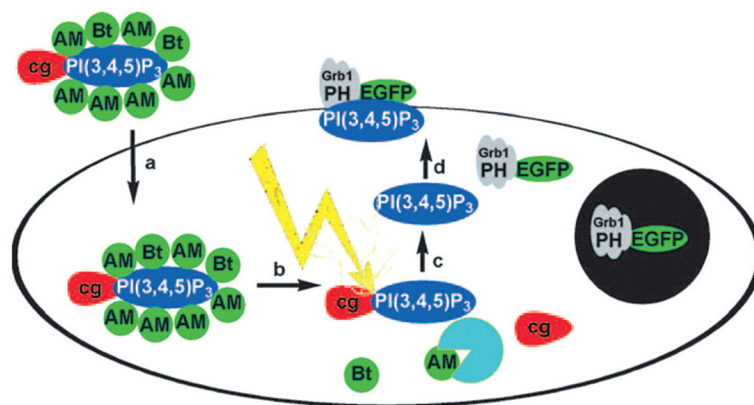
Fig. 5.
Mechanism of action of PI(3,4,5)P$_3$: (a) cell entry; (b) enzymatic removal of Bt and AM protecting groups produces cgPI(3,4,5)P3; (c) light-induced removal of coumarin protecting group; (d) PI(3,4,5)P3 induces translocation of EGFP-Grp1-PH domains to the plasma membrane.[67]
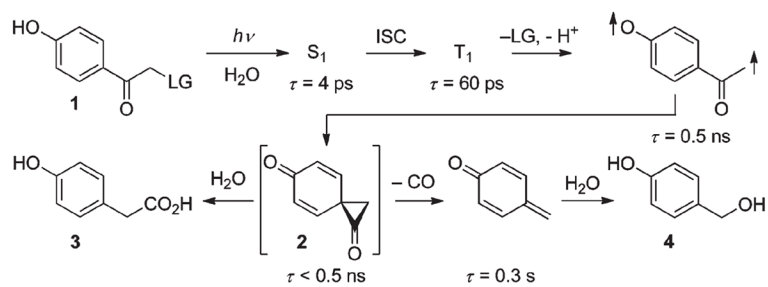
Scheme 1.
Mechanism for pHP photoisomerization and leaving group (LG) release.[8]
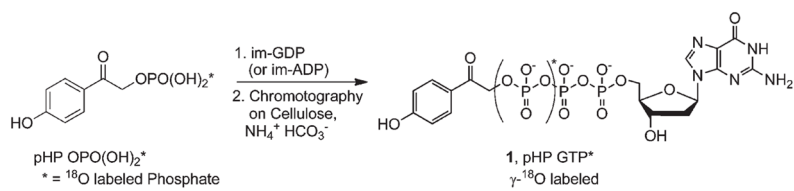
Scheme 2.
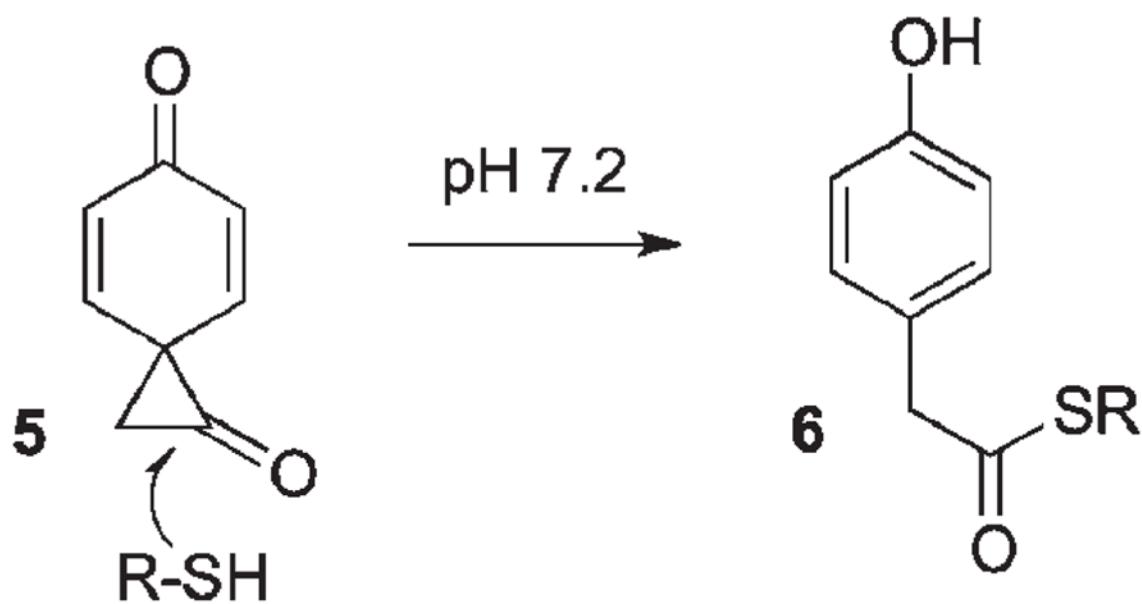
Scheme 3.
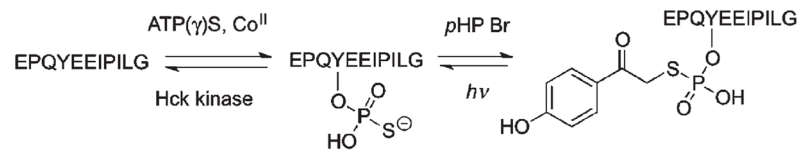
Scheme 4.
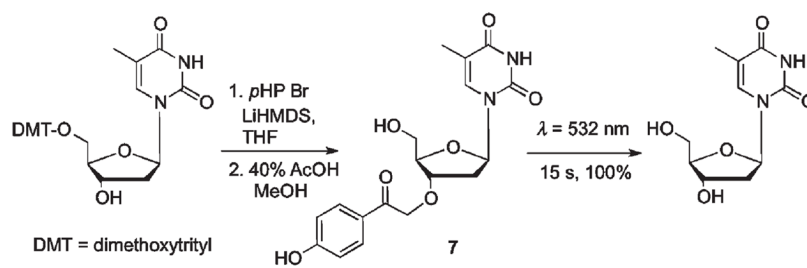
Scheme 5.
Synthesis and release of *p*HP caged thymidine **7**.
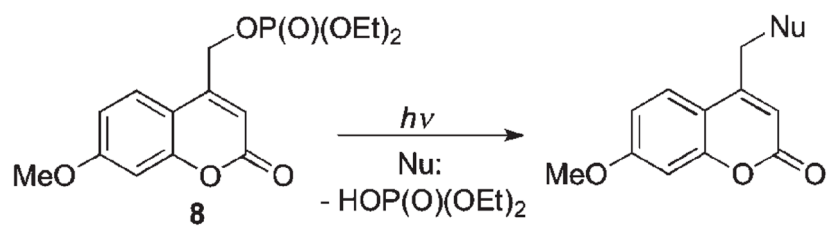
Scheme 6.
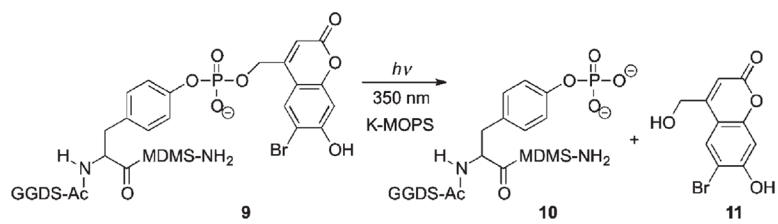
Scheme 7.
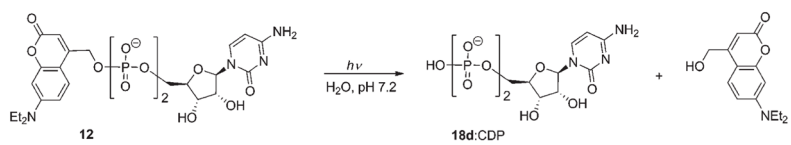
Scheme 8.

Scheme 9.

Scheme 10.

	X	Y	Φ_{ax}	Φ_{eq}
a	H	H	0.085	0.055
b	OMe	H	0.03	0.02
c	H	OMe	0.13	0.07
d	OMe	OMe	0.04	0.04
e	H	NMe$_2$	0.28	0.26
f	H	NEt$_2$	0.21	0.23

Scheme 11.

19a (X = H, Y = N(CH$_2$CO$_2$H)$_2$)
19b (X = Y = OCH$_2$CO$_2$H)

Pur =

adenin-9-yl   guanin-9-yl   8-bromoadenin-9-yl   8-bromoguanin-9-yl

Scheme 12.

21 (R = Me)

22a (R = H)
22b (R = Me)

23

24
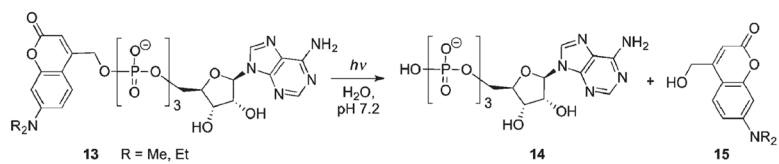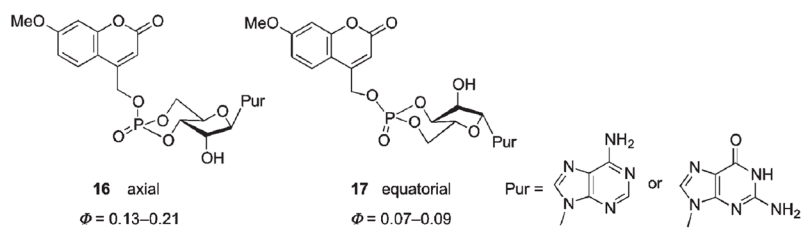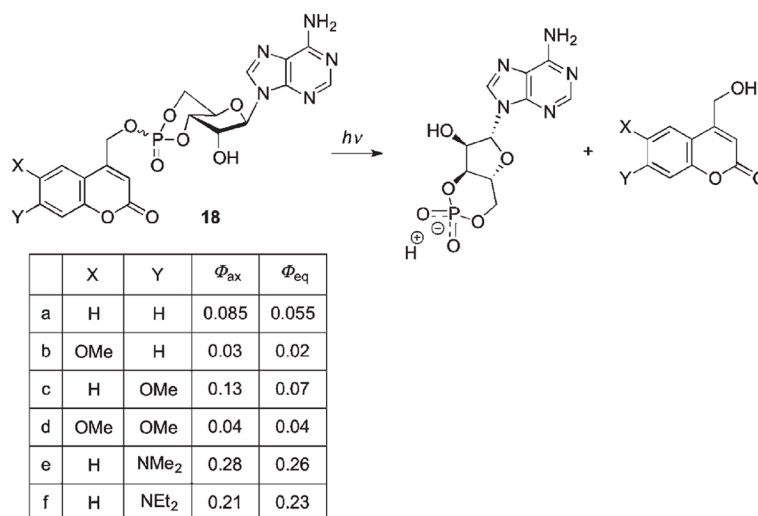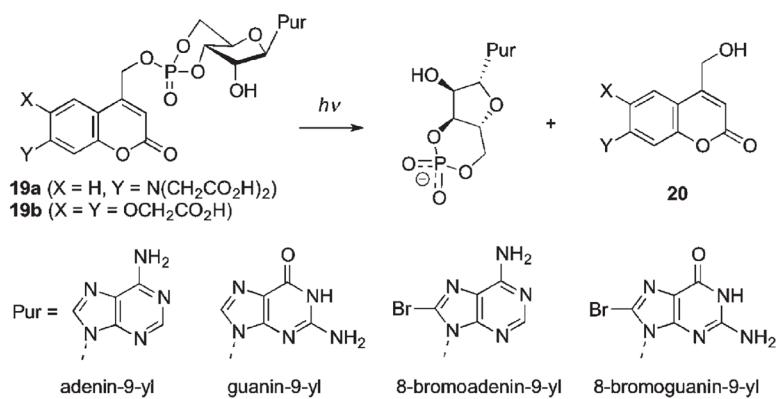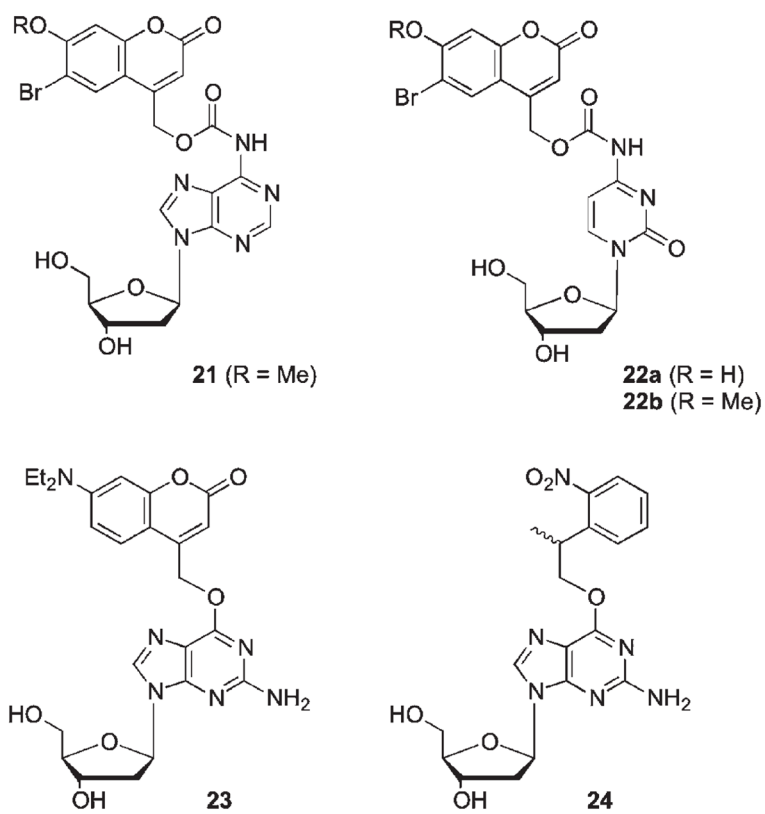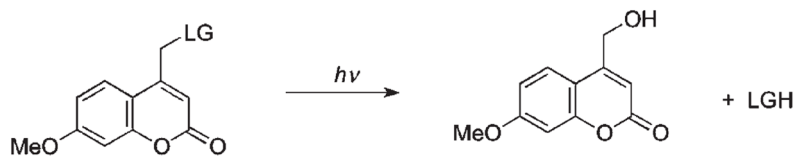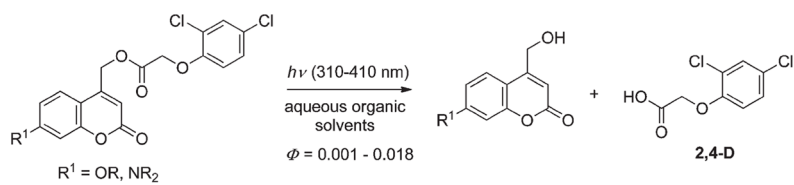
Scheme 13.

Scheme 14.

Scheme 15.
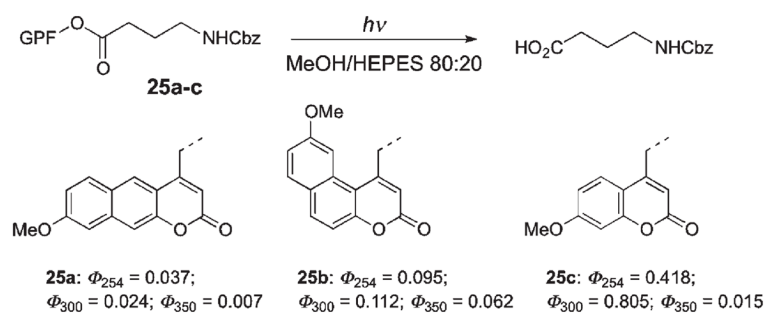
Scheme 16.
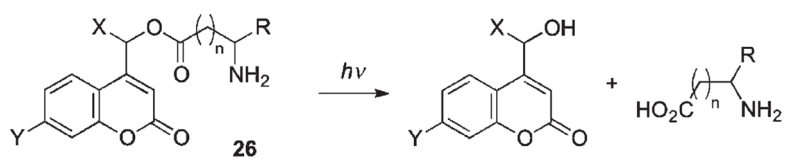
Scheme 17.
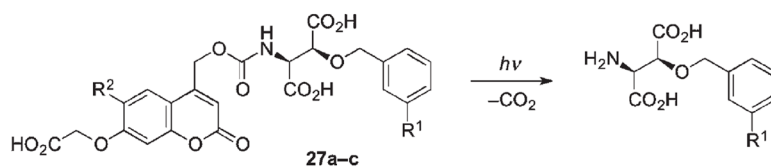
27a: $R^1 = R^2 = H$
27b: $R^1 = H$, $R^2 = OCH_2CO_2H$
27c: $R^1 = p\text{-}CF_3C_6H_4CONH$, $R^2 = OCH_2CO_2H$

Scheme 18.

28: R = PhCH₂, X = O
29: R = CO₂Me, X = H₂

30

31
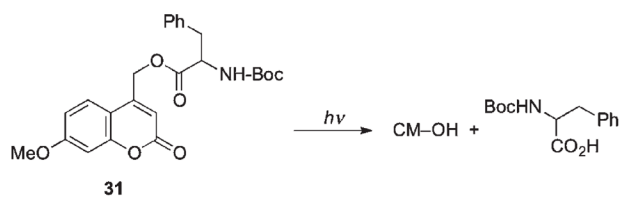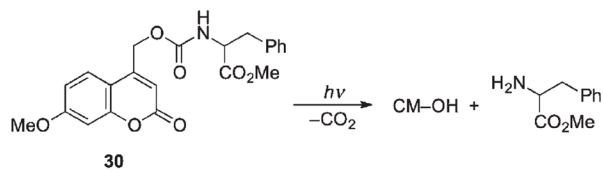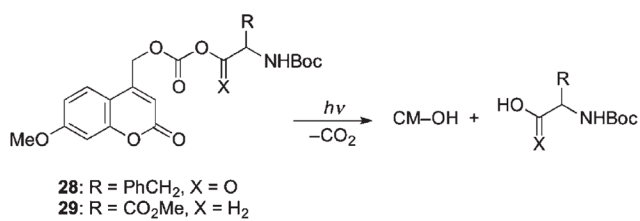
Photolysis rate constants $k/(10^{-2}\ min^{-1})$:

	254 nm	300 nm	350 nm
28	10.41	7.21	0.14
29	1.94	2.81	0.05
30	4.97	4.59	0.07
31	8.92	3.99	0.10

Scheme 19.
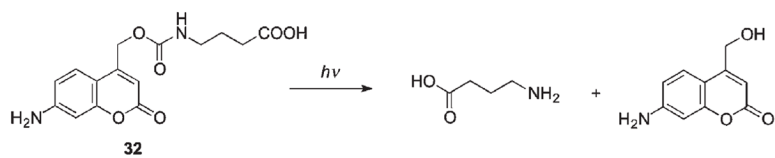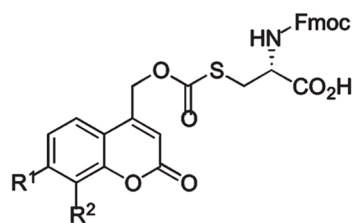
Scheme 20.
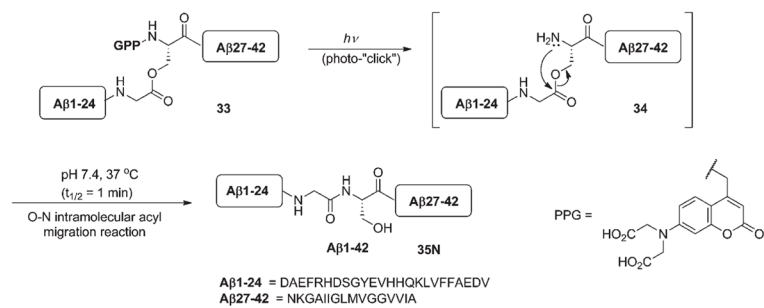
Scheme 21.
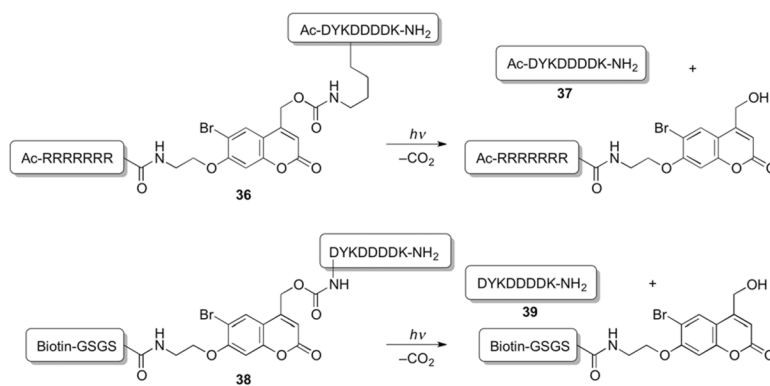
Scheme 22.
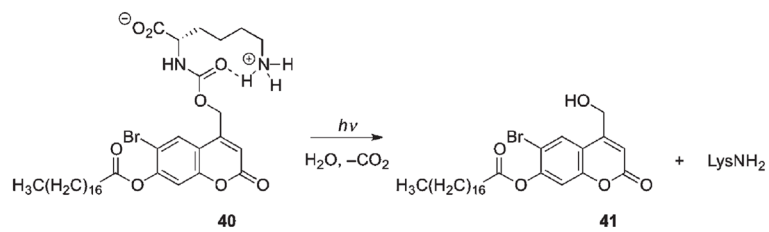
Scheme 23.
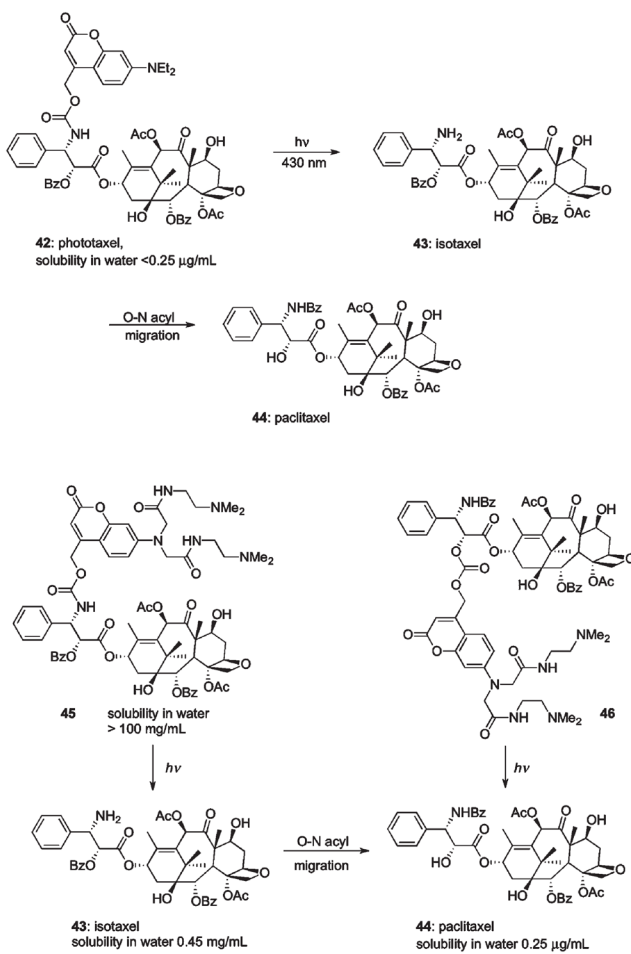
Scheme 24.

Scheme 25.

Scheme 26.

Ac-Cys(**49**)-Val-Thr-Gly-Ala-Pro-Gly-Cys(**50**)-Val-Gly-Gly-Gly-Arg-Leu-NH$_2$

$h\nu$, $\lambda_{irr} \geq 402$ nm
dithiotheriol (10 equiv.)

Ac-Cys-Val-Thr-Gly-Ala-Pro-Gly-Cys(**50**)-Val-Gly-Gly-Gly-Arg-Leu-NH$_2$

+

Ac-Cys(**50**)-Val-Thr-Gly-Ala-Pro-Gly-Cys-Val-Gly-Gly-Gly-Arg-Leu-NH$_2$ + **49**

$h\nu$, $\lambda_{irr} \geq 325$ nm

Ac-Cys-Val-Thr-Gly-Ala-Pro-Gly-Cys-Val-Gly-Gly-Gly-Arg-Leu-NH$_2$ + **50**
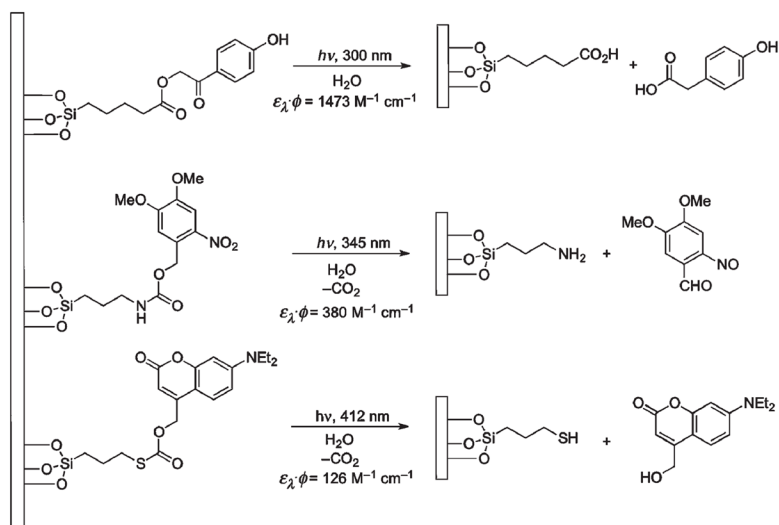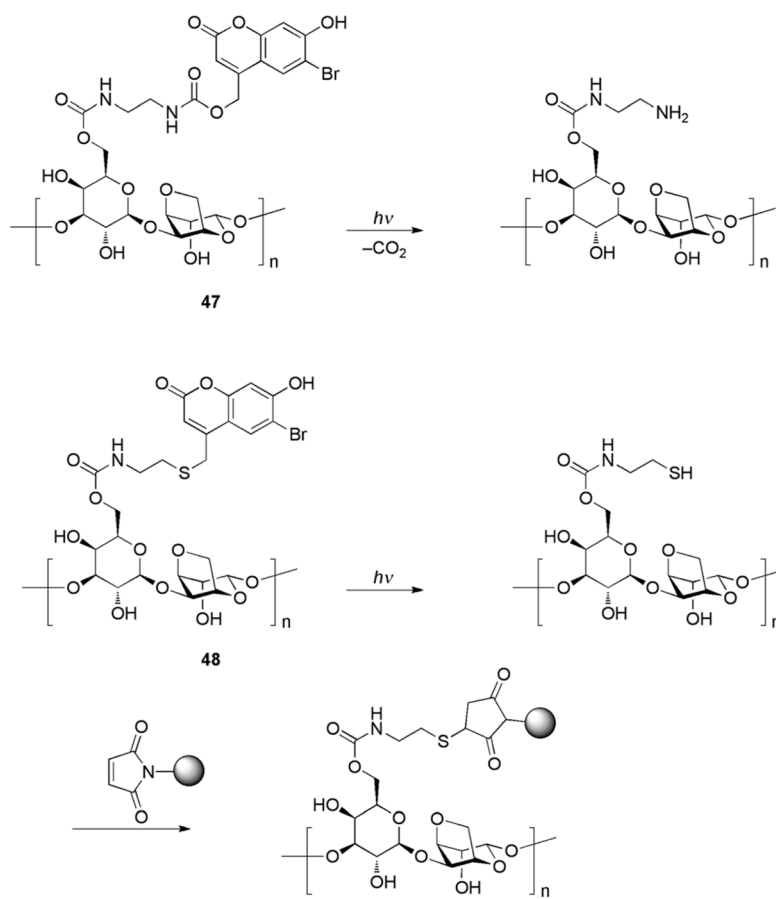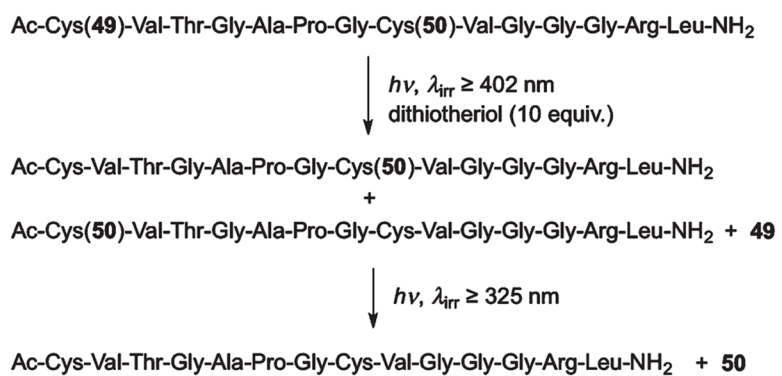
49: R^1 = N(CH$_2$CO$_2$H)$_2$, R^2 = H
50: R^1 = R^2 = N(CH$_2$CO$_2$H)$_2$

Scheme 27.

51a–d   **51a** R^1 = MeO, R^2 = H; **51b**: R^1 = OH, R^2 = Br;
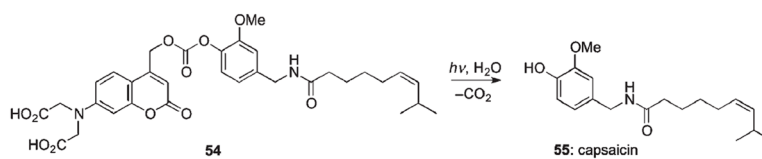   **51c**: R^1 = Et$_2$N, R^2 = H; **51d**: R^1 = R^2 = MeO
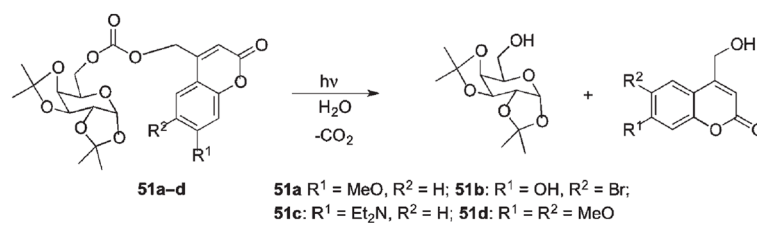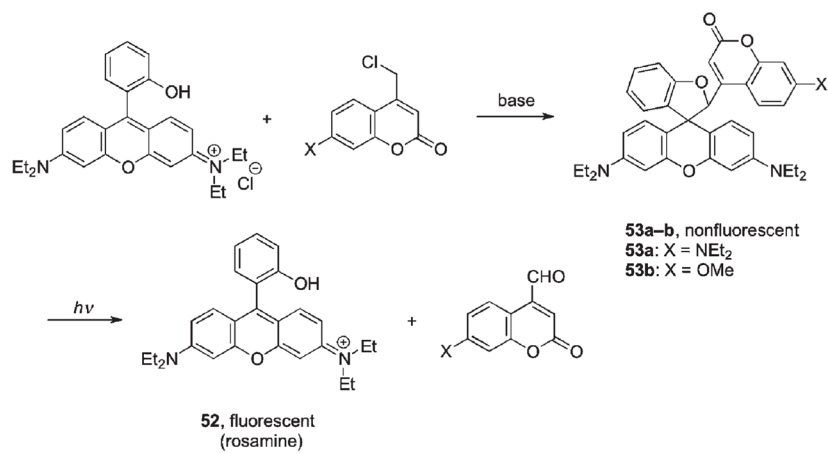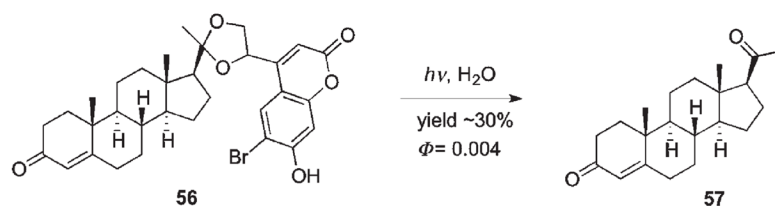
Scheme 28.

Scheme 29.

Scheme 30.

Scheme 31.

Table 1
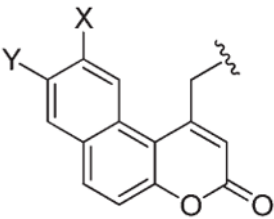
Representative pK_a's, disappearance quantum yields of pHP derivatives (Φ_{dis}), triplet state lifetimes ($^3\tau$), and rate constants for the release of the leaving groups (LG) calculated as $k_{rel} = \Phi_{dis}/^3\tau$ [11–13]

LG	pK_a [12] (LG)	Φ_{dis} [13]	$^3\tau$/ns [11]	$\log(k_{rel}/s^{-1})$
Mesylate	−1.54	0.932	0.118	9.70
Tosylate	−0.43	1.04	0.104	10.0
Diethyl phosphate	0.71	0.40	0.345	9.06
p-CF$_3$ benzoate	3.69	0.201	0.625	8.51
Formate	3.75	0.94	0.667	9.15
p-OCH$_3$ benzoate	4.09	0.288	0.833	8.54
Benzoate	4.21	0.316	1.16	8.44
GABA	4.76	0.21	0.345	8.78
p-CN phenolate	7.17	0.11	1.45	7.88
Phenolate	9.8	0.04	3.85	7.02

Table 2

Typical coumarin chromophores

λ_{max}	Structure	Abbreviation	Solvent[a]	Ref.
320–330 nm		HCM (R = H)	C	40
			D	41
		7-MCM, Bpm (R = Me)	C	40,42
			F	43
			A,D	38,41,44
		CMCM (R = CH$_2$CO$_2$H)	D	45
330–380 nm		DMCM (X = Y = OMe, Z = H)	F	43
			A	38,46
		BCMCM (X = Y = OCH$_2$CO$_2$H, Z = H)	D	45
			B	47
		7,8-BCMCM (X = H, Y = Z = OCH$_2$CO$_2$H)	G	48
		BHCM, Bhc (X = Br, Y = OH, Z = H)	E	49,50
			G	51
			F	43
		BMCM (X = Br, Y = OMe, Z = H)	E	49
		BBHCM (X = Br, Y = OH, Z = N(CH$_2$CO$_2$Bu^t)$_2$) (X = Br, Y = n-C$_{17}$H$_{35}$CO$_2$, Z = H)	G	51
			B	52
350–400 nm		ACM (R = H)	D	41
		DMACM (R = Me)	B	53
			A	38,44
		DEACM (R = Et)	H,B	54–57
			D	58
			F	43
			A	38,46
		BCMACM (R = CH$_2$CO$_2$H)	B	59,60
			D	
		BBCMACM (R = CH$_2$CO$_2$Bu^t)	G	61
340–360 nm		Obb (X = H) Bbl (X = MeO)	C	42,62

λ_{max}	Structure	Abbreviation	Solvent[a]	Ref.
		Obc (X = OH, Y = H) Obm (X = OMe, Y = H) Bba (X = H, Y = OMe)	C	42,62,63

[a]Solvents: HEPES–MeOH (A); HEPES buffer (B); EtOH (C); PB or PBS buffer (D); KMOPS buffer (E); KMOPS–MeOH (F); HEPES–MeCN (G); water (H).

Table 3

Effect of pK_a on quantum yields and cleavage rate constants k_{cl}[38]

LG	pK_a	$\Phi/10^{-3}$	$k/10^9$ s^{-1}
$C_6H_{13}CO_2^-$	4.89	4.3	0.32
p-CH_3O–$C_6H_4CO_2^-$	4.41	4.5	0.20
$C_6H_5CO_2^-$	3.99	5.2	0.18
p-CN–$C_6H_4CO_2^-$	3.54	6.4	4.0
$^-OP(O)(OEt)_2$	0.71	37	6.6

Table 4

Photorelease of coumarylmethyl-caged neurotransmitters

	Y	X	LG	λ/nm (pH)	Φ	Ref.
26a	$N(CH_2CO_2H)_2$	H	GABA	380 (7.2)	0.2	2
26b	$N(CH_2CO_2H)_2$	H	Glu	380 (7.2)	0.1	2
26c	$N(CH_2CO_2H)_2$	H	Phe	— (7.2)	—	71
26d	NEt_2	H	Gly	400 (7.4)	0.12	55
26e	NEt_2	H	Glu	400 (7.4)	0.11	28
26f	NEt_2	H	GABA	400 (7.4)	0.14	29
26g	NEt_2	a	GABA	400 (7.4)	0.1	55

[a] $X = -CONH-CH_2-CO_2Et$.